

## Article

# Trends, Atmospheric Patterns, and Spatial Variability of Heatwaves in an Oceanic Climate Area of NW Iberia

Luis Pérez-García \*, Cristina García-Hernández  and Jesús Ruiz-Fernández 

Department of Geography, University of Oviedo, C/ Amparo Pedregal s/n, 33011 Oviedo, Asturias, Spain; garciacristina@uniovi.es (C.G.-H.); ruizjesus@uniovi.es (J.R.-F.)

\* Correspondence: uo296491@uniovi.es

**Abstract:** In the Atlantic region of northern Spain, heat extremes were historically rare, but in recent decades, they have become more intense and persistent. This article characterizes heat events in Asturias (NW Spain) between 2001 and 2023, focusing on their frequency, intensity, and duration, as well as their temporal trends. Additionally, it explores the synoptic patterns linked to these episodes to enhance understanding of their occurrence and evolution over the study period. The research is based on official meteorological records, and it distinguishes between officially declared heatwaves (DHs) and significant heat events (SHEs) identified through regional press reports. This methodology enables the study to capture a broader spectrum of heat-related impacts. During the study period, 17 episodes were documented (11 DHs and 6 SHEs). The frequency, intensity, and duration of heat events have significantly increased, particularly since 2016, standing the last two years (2022 and 2023). Both DHs and SHEs have progressively shifted toward the early and late periods of the astronomical summer, with some events occurring during spring and autumn in the second half of the study period (years 2017, 2022, and 2023). Three atmospheric patterns have been identified as responsible for extreme heat episodes; Type 1 (warm tropical continental air masses, combined with atmospheric stability) is responsible for 10 of the episodes. Furthermore, urban areas and main river valleys were the most affected areas, while coastal regions remained largely unaffected. This research aims to contribute to a broader understanding of how heatwaves are evolving in a temperate climate area under the influence of global warming, providing insights to inform and improve adaptation strategies for mitigating their impacts.

**Keywords:** heatwaves; climate change; temperature anomalies; climate extreme; oceanic climate



Academic Editors: Shady Attia, Zhengxuan Liu, Baojie He and Ali Cheshmehzangi

Received: 20 December 2024

Revised: 18 January 2025

Accepted: 22 January 2025

Published: 2 February 2025

**Citation:** Pérez-García, L.; García-Hernández, C.; Ruiz-Fernández, J. Trends, Atmospheric Patterns, and Spatial Variability of Heatwaves in an Oceanic Climate Area of NW Iberia. *Land* **2025**, *14*, 310. <https://doi.org/10.3390/land14020310>

**Copyright:** © 2025 by the authors. Licensee MDPI, Basel, Switzerland. This article is an open access article distributed under the terms and conditions of the Creative Commons Attribution (CC BY) license (<https://creativecommons.org/licenses/by/4.0/>).

## 1. Introduction

Heatwaves are a climatic hazard with significant global consequences in terms of both economic losses and human fatalities. Vulnerable groups, such as the elderly, young children, and individuals with chronic illnesses, are particularly susceptible to health complications during these events [1]. Outdoor workers and those lacking cooling systems are especially prone to heat stress, a risk further exacerbated by urbanization and limited access to green spaces [2–4].

The intensity, frequency, and duration of heatwaves have increased globally, a trend that is expected to accelerate as global warming progresses [5]. This will likely worsen their impacts on human health [6] and biodiversity [7]. In Southern European countries, climate change has amplified these extreme phenomena since the early 21st century. For instance, major capitals have seen a rise in the number and duration of

heatwave days [8]. In the Western Mediterranean, heatwaves in 2022 and 2023 reached unprecedented temperature anomalies of up to +3.6 °C, exceeding climatic variability observed over the past millennium [9]. During this period, losses in workdays, hospitalizations, and heat-related fatalities increased significantly, resulting in severe social and economic impacts [10].

Heat extremes have equally grown in frequency, duration, intensity, and spatial extent in the Iberian Peninsula since the mid-20th century, with the most severe events concentrated after 1985 [11], and particularly severe events during the early summers of the 2020s [9]. Recent studies project that heatwave-related deaths in Spain could increase by 292% during 2031–2080 compared to 1971–2010 [12]. Beyond health impacts, heatwaves harm the most sensitive ecosystems and reduce the availability of water, a relatively scarce resource in the country [13,14]. Furthermore, critical sectors such as tourism and agriculture are highly vulnerable to the increasing frequency of these extreme events [15–17].

In Asturias, an oceanic climate region located in northern Spain, the proximity of the Cantabrian Sea has historically granted mild temperatures, with heatwaves being relatively infrequent compared to other Spanish sectors. However, the northern half of the Iberian Peninsula experienced significant increases in heatwave severity (in terms of frequency and intensity) between 1950 and 2019 [11], and projections indicate that, in this region, heatwave-related mortality rates could exceed 13.4 deaths per 1000 inhabitants/year during the 2021–2050 period [18]. The increasing likelihood of heatwaves becoming a frequent occurrence in regions like Asturias in the coming years makes it imperative to deepen our understanding of these events in order to enhance both our resilience and adaptive capacities.

In terms of scientific production on this topic, it is noteworthy that, to date, most studies related to heatwaves have focused on Mediterranean regions of Europe or the Iberian Peninsula. In contrast, regions with an oceanic climate have been relatively unexplored, as this phenomenon is less frequent in such areas. Consequently, there is a paucity of the literature directly comparable to our study. However, there are numerous examples of studies on recent heatwaves occurring worldwide. Notable examples include cases in South America, such as those in Brazil (2020) and Peru (2016) [19], as well as in the Western United States and Canada in June 2021 [20]. In Europe, the most significant extreme heat events have taken place over the past three decades, with particularly notable instances in 2003 and 2015 [21], 2019 [22], and 2021 [23].

Given the preceding considerations, the main goal of this research is to describe the nature of heatwaves in Asturias and examine how they have changed over the past two decades, between 2001 and 2023. Specifically, the study seeks to address the following objectives:

- (i) To examine the characteristics (frequency, intensity, and duration) of extreme heat events that occurred in Asturias between 2001 and 2023.
- (ii) To assess the temporal trends of extreme heat events over the study period.
- (iii) To identify the synoptic patterns associated with the occurrence of extreme heat events in the region.

## 2. Data and Methods

This study draws upon documentation prepared by the Spanish State Meteorological Agency (AEMET), which provides detailed records of all officially recognized heatwaves in Spain from 1975 to 2023. The criterion used by AEMET to identify declared heatwaves (DHs) is the following: exceeding the 95th percentile of maximum temperature for a specific date and location compared to the average for a 30-year reference period (specifically, the 1971–2000 reference period). This condition must occur in at least 10% of the stations and persist for a minimum of three consecutive days. The meteorological stations used to determine official



heatwaves in Spain total 137, meeting requirements such as uniform territorial distribution, current operational status, and sufficiently long data series to calculate percentiles. Thus, in Asturias, only two observatories are used as references: the Oviedo/Uviéu station and the Asturias Airport station. These documentations from AEMET include key parameters such as the start and end dates of each event, their duration in days, the maximum temperature reached, the temperature anomaly, and the geographical areas affected ([https://www.aemet.es/es/conocerlas/recursos\\_en\\_linea/publicaciones\\_y\\_estudios/estudios/detalles/olascalor](https://www.aemet.es/es/conocerlas/recursos_en_linea/publicaciones_y_estudios/estudios/detalles/olascalor). Accessed on 5 November 2023). Using this dataset, heatwave episodes occurring in Asturias during the period from 2001 to 2023 were specifically selected for a further analysis.

Additionally, information was extracted from news reports using the digital archives of the regional newspapers *El Comercio* and *La Nueva España*. The analysis covered the period from 1 January 2001 to 31 December 2023 (a total of 23 complete years). Key terms such as “heatwave”, “extreme heat”, “scorching heat”, “extreme temperatures”, and “intense heat” were entered into the search engines. The selection of these terms—some of which are highly colloquial but commonly used by the local Asturian press when addressing these events—was informed by a preliminary review of news articles, where their frequent occurrence was noted. This facilitated the identification of additional extreme heat episodes. The extracted information includes both quantitative data (maximum temperatures recorded and the impacts of heat on populations and assets) and qualitative insights (public perceptions of heat-related effects). For data prior to 2006, digital archives were unavailable in virtual newspaper repositories and were instead accessed through digitized records held in the archives of the Central Library of Asturias.

The primary objective of analyzing press reports is to identify additional warm episodes beyond the officially declared heatwaves recognized by the national meteorological service. In this context, the study has considered all warm events reported by the press as significant in terms of perceived impact, even if they do not meet the official criteria for classification as a heatwave. This approach acknowledges that such events also illustrate the effects of high temperatures on populations and their activities. A clear distinction has been made between “declared heatwaves” (DHs), as officially recognized by AEMET, and unofficially recognized heat episodes, referred to as “significant heat events” (SHEs). The DHs have been identified based on the documentation from AEMET, which annually records the heatwaves occurring in Spain according to the three official criteria mentioned earlier (95th percentile of maximum temperatures, lasting at least 3 days and affecting at least 10% of the territory). This documentation specifies the territorial extent of each heatwave in Spain, allowing for the selection of DH affecting Asturias. The information on these events was supplemented using reports from the local written press. The SHEs were identified from press reports based on the fulfillment of three essential criteria. Specifically, for an event to be classified as an SHE, it must meet the following conditions: (i) the existence of, at least, two separate new items describing the effects of extreme heat; (ii) the presence of consistent information regarding the event in reports from two distinct media outlets; (iii) the reported heat conditions must have persisted for a minimum of two consecutive days.

This study applies basic descriptive statistical methods to analyze the data, including the generation of graphs and tables. Synoptic maps obtained from the German website *Wetterzentrale* provided numerical and cartographic data on atmospheric conditions at various levels (<https://www.wetterzentrale.de/es/reanalysis.php?map=1&model=avn&var=1>. Accessed on 5 November 2023). The *Wetterzentrale* maps are derived from reanalysis data produced by the Global Forecast System (GFS) of the United States National Weather Service and the National Oceanic and Atmospheric Administration (NOAA). For this analysis, maps were selected to depict atmospheric conditions at 500 hPa, 850 hPa, and sur-

face levels, corresponding to the warm episodes and heatwaves detected in Asturias. This methodology facilitated a comprehensive understanding of the synoptic patterns associated with these events. These were supplemented with cartography produced using QGIS version 3.14.16, integrating a municipal-level base map sourced from the Download Center of the Autonomous Agency “Centro Nacional de Información Geográfica” (CNIG) (<https://centrodedescargas.cnig.es/CentroDescargas/home>. Accessed on 5 November 2023).

### Study Area

Asturias, situated in the Northwestern region of the Iberian Peninsula, corresponds geographically to the Asturian Massif. This geological structure, primarily composed of sedimentary and metamorphic rocks from the Paleozoic Era, forms the highest segment of the Cantabrian Mountains. The topography of this area exhibits a progressive increase in elevation from the Cantabrian Sea towards the south, where uplands frequently exceed 2000 m. This landscape is characterized by sharp altitudinal gradients, steep slopes, and narrow valleys. The climate in Asturias varies significantly due to its complex orography and geographical positioning (Figure 1). According to the Köppen–Geiger classification [24], the majority of Asturias falls within the Cfb climate zone (Temperate Oceanic), characterized by temperate conditions with mild summers and abundant rainfall throughout the year. In contrast, the southwestern portion of the region experiences a Csb climate, featuring warmer, drier summers typical of Mediterranean influences. Elevational increases bring about a transition to the Df climate zone, characterized by colder temperatures and significant winter precipitation. Based on AEMET data, Asturias has an average annual temperature of approximately 14 °C, with 2023 recording a slightly higher average of 14.7 °C. The region receives an average annual precipitation of 1259 mm, as calculated over the 1991–2020 reference period.

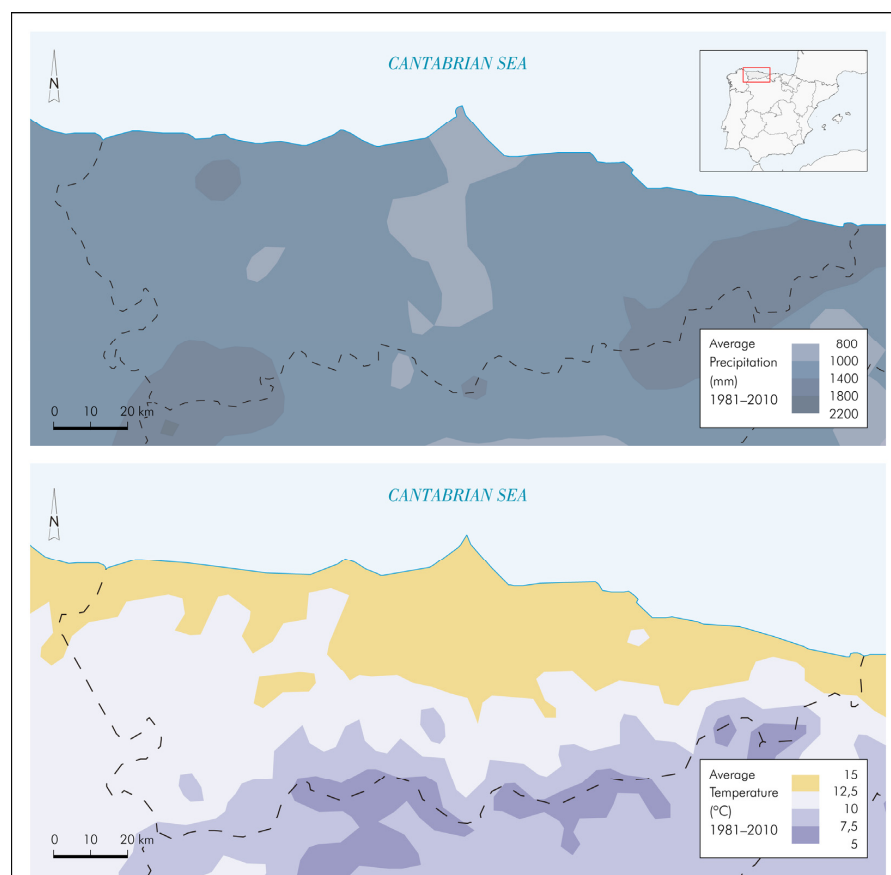
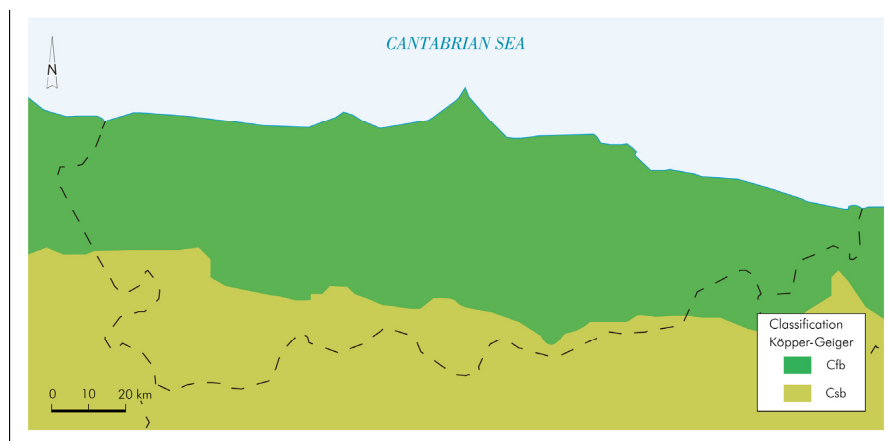


Figure 1. Cont.



**Figure 1.** Climate context of Asturias: mean temperature, mean precipitation, and Köppen–Geiger classification. Source: Modified from Atlas Nacional de España (ANE) CC BY 4.0 ign.es and Olivares-Navarro [24].

### 3. Results

#### 3.1. Overview and Temporal Trends of Extreme Heat Events During Study Period

##### 3.1.1. Interannual Evolution

According to the official records from AEMET, 11 DHs have occurred in Asturias since 2001. However, this study identified 6 additional SHEs based on the criteria outlined in the methodology, resulting in a total of 17 episodes during the study period (Table 1). During all six episodes in Asturias, the maximum temperature thresholds corresponding to the 95th percentile were not exceeded at either of the two observatories considered by AEMET to determine official heatwaves, namely Oviedo/Uviéu and Asturias Airport. Therefore, although all these episodes lasted long enough, they cannot be classified as official heatwaves due to the thresholds not being reached at these meteorological stations. However, following the criteria outlined in the methodology, these episodes have been considered as they had adverse effects reported by the local press.

**Table 1.** Episodes of extreme heat (DH/SHE) occurring in Asturias during the analyzed period, indicating the dates, duration, and maximum temperatures, as well as the municipality where they were recorded. Source: Own work.

Year	Start Date	End Date	Duration (Days)	T. Max (°C)	Municipality	Type
2003	3 August 2003	13 August 2003	11	35.6	Uviéu	DH
2006	16 July 2006	18 July 2006	3	38.9	Ibias	SHE
2006	4 September 2006	6 September 2006	3	33	Cangues O.	DH
2011	25 June 2011	27 June 2011	3	36.5	Tinéu	SHE
2012	8 August 2012	11 August 2012	4	38.1	Tinéu	DH
2016	17 July 2016	19 July 2016	3	38.5	Mieres	DH
2016	5 September 2016	7 September 2016	3	36.5	Ibias	DH
2017	18 June 2017	21 June 2017	4	36	Ibias	DH
2017	20 August 2017	22 August 2017	3	37	Cangas N.	DH
2018	2 August 2018	6 August 2018	5	36.7	Ibias	SHE
2020	5 August 2020	7 August 2020	3	37.5	Amieva	SHE
2022	15 June 2022	17 June 2022	3	39.5	Cabrales	DH
2022	9 July 2022	18 July 2022	10	41.4	Mieres	DH
2022	10 August 2022	12 August 2022	3	35.4	Tinéu	SHE
2023	8 August 2023	10 August 2023	3	38	Somiedo	DH
2023	22 August 2023	24 August 2023	3	40.3	L.lena	DH
2023	7 October 2023	12 October 2023	6	35	Mieres	SHE

Regarding frequency, the number of recorded episodes exhibits an increasing trend, with a clear concentration of events in the final third of the study period (Figure 2). This final third, beginning in 2016, accounts for 12 of the 17 identified episodes, while 3 episodes occurred in the first third (2000–2007) and 2 in the second third (2008–2015). Within this final third, some years experienced up to three episodes annually, as observed in 2022 and 2023. In terms of differences in frequency between DHs and SHEs, the former have been more common, with 11 DHs compared to 6 SHEs. Although DHs have generally been more frequent, there are years, such as 2003, 2012, 2016, and 2017, where the number of each type of episode is identical. Notably, SHEs occurred without accompanying DHs in 2011, 2018, and 2020 (Figure 2).

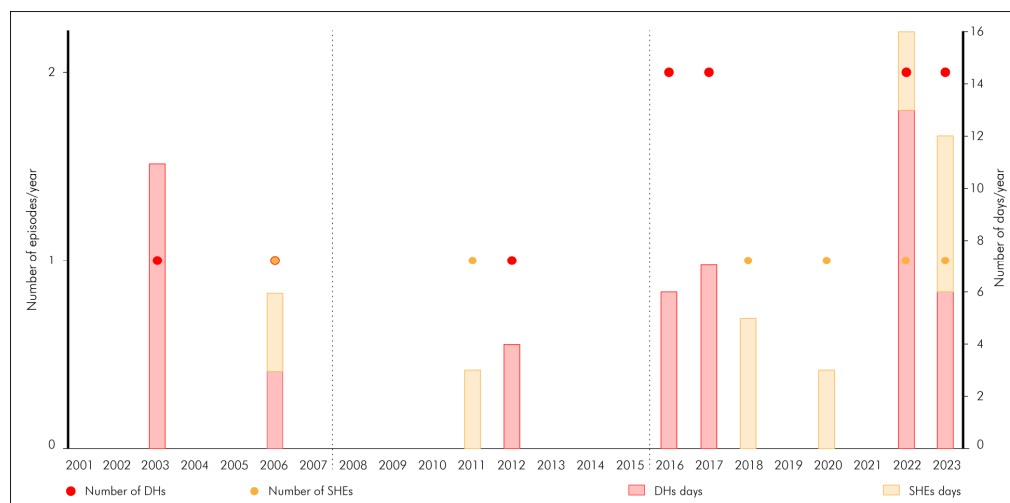


**Figure 2.** Number of DHs, number of SHEs, and annual days under both types of extreme heat events (DH + SHE) for period between 2001 and 2023. Source: Own work.

The duration of episodes shows a general increasing trend over the study period. Collectively, the episodes spanned a total of 73 days; however, the distribution is notably uneven. Of these, 49 days occurred in the final third of the period, starting in 2016 (Figure 2), while 17 days were recorded in the first third and 7 in the second. It is worth noting that in the first third, 11 of the 17 days correspond to a single heatwave (August 2003), whereas in the final third, the total number of days is distributed across a greater number of episodes. Specifically, in 2022 and 2023, a combined total of 28 extreme heat days were recorded, resulting from three separate episodes in each year (Figure 3). The average duration of episodes was 4.3 days, with the most common length being 3 days (11 occurrences), followed by 4 days (2 occurrences). Once again, the last two years of the series (2022 and 2023) stand out, concentrating the highest number of days with three episodes per year and average durations of 5.3 and 4 days per episode, respectively. As a notable exception, 2003 accumulated a high number of days within a single event (11 days).

The intensity of the episodes also shows an increasing trend throughout the study period. It was in the last third of the period when the barrier of 40 °C was surpassed in two episodes and when the average of the maximum temperatures reached was higher, with 35.42 °C compared to 34.29 °C on average during the episodes of the second third and 33.45 °C on average during the first third. In general, the intensity is greater in DH events than in SHEs, with average maximum temperatures of 35.27 °C and 34.32 °C, respectively.

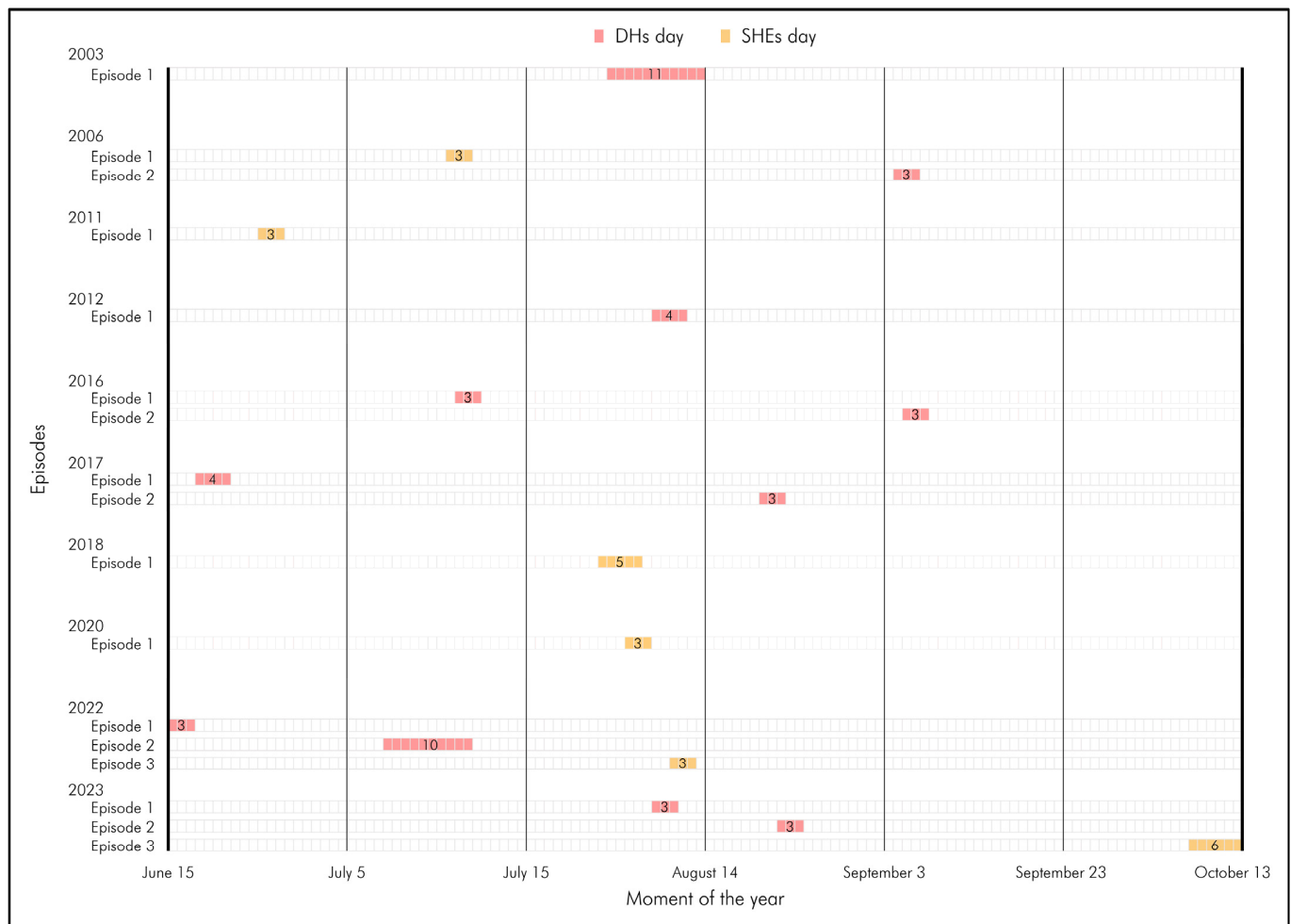


**Figure 3.** Start and end dates of each episode (DH/SHE) recorded in Asturias during the period from 2001 to 2023. Source: Own work.

### 3.1.2. Intra-Annual Evolution

Concerning the months in which the events occur, of the seventeen identified episodes, eight took place in August, three in June, and three in July, while two occurred in September and one in October. The highest concentration of events has been observed in the first half of August (Figure 3), and this pattern has remained relatively consistent over the past 20 years. However, a potential trend is the gradual shift in both DHS and SHEs toward the beginning and end of the astronomical summer, with some episodes in recent years extending beyond this period.

The first instance of such an occurrence was in 2017, when a DH began in late spring, specifically on June 18 (Figure 3). This phenomenon was repeated in the summer of 2022, with the first heatwave starting even earlier, on June 15. The following year, in 2023, marked the first time an SHE occurred in October, during the astronomical autumn. Overall, the annual window during which these episodes take place may have been progressively expanding, with some events now occurring in both spring and autumn, a trend that became more pronounced in 2022 and 2023.

### 3.2. Synoptic Conditions During Each Extreme Heat Episode

Three main atmospheric patterns have been identified as the drivers of the DHS and SHEs that occurred in Asturias during the study period. Table 2 summarizes these three primary atmospheric configurations associated with extreme heat conditions in the region. The most frequent pattern, Type 1, is observed in 10 of the 17 analyzed episodes. This



pattern involves the advection of a warm air mass of a continental tropical (Tc) origin from Africa, encompassing the entire Iberian Peninsula at the 850 hPa level. At the surface, conditions are stable under the influence of the Azores High, while at higher altitudes (500 hPa), a ridge is positioned over the peninsula. The advection of the warm air mass is driven by southerly winds at upper levels, facilitated either by a trough located over the Atlantic or by the counterclockwise circulation of a cut-off low.

**Table 2.** An illustration of the typical situations that cause warm episodes in Asturias. Source: Own work.

Type of Situation	Atmospheric Configuration	Number of Episodes	DH	SHE
Type 1	Advection of warm air mass (Tc) from Africa	10/17	8/10	2/10
Type 2	Advection of warm air mass (Tm) from the Atlantic Ocean	5/17	2/5	3/5
Type 3	Persistent stability	2/17	1/2	1/2

One of the clearest examples of this situation is the heatwave that occurred between 9 and 18 July 2022. While most episodes fit this Type 1 classification (Table 3), this pattern is more commonly associated with DHs and occurs less frequently in the case of SHEs (Table 2).

**Table 3.** A summary of the key values of each atmospheric configuration responsible for the 17 DH/SHEs that occurred in Asturias between 2001 and 2023. Source: Own work.

Date	Geopot. 500 hPa (m)	Temp. 850 hPa (°C)	Pressure Sup. (hPa)	Trough/Cut-Off Low	Position of the Trough	Type
3–13 August 2003	5920	25	1015	YES	Azores	1
16–18 July 2006	5800	20	1015	YES	West UK	1
4–6 September 2006	5960	22	1015	YES	Iceland–West Azores	2
25–27 June 2011	5920	20	1015	YES	West UK	2
8–11 August 2012	5960	24	1015	YES	East of Azores	1
17–19 July 2016	5840	25	1015	YES	South of Iceland. East of Azores	1
5–7 September 2016	5880	26	1015	YES	Azores–UK	1
18–21 June 2017	5920	22	1020	NO	-	3
20–22 August 2017	5920	23	1015	YES	West UK	2
2–6 August 2018	6000	22	1020	NO	-	3
5–7 August 2020	5880	22	1015	YES	West UK	2
15–17 June 2022	5840	20	1015	YES	Lisbon–Azores	1
9–18 July 2022	5920	29	1015	YES	Lisbon–Azores	1
10–12 August 2022	5880	20	1015	YES	Lisbon–Azores	1
8–10 August 2023	5960	24	1015	YES	Southeastern Azores	1
22–24 August 2023	5960	28	1015	YES	Northeastern Azores	1
7–12 October 2023	5880	18	1025	YES	North Azores	2

The Type 2 configuration accounts for five extreme heat episodes. This pattern involves the advection of a warm air mass at the 850 hPa level from the Atlantic Ocean, classified as tropical maritime (Tm). This air mass is transported toward the Iberian Peninsula by southwesterly winds at upper levels, driven by the positioning of a trough and/or a cut-off low over the Atlantic and a ridge over Spain at the 500 hPa level. The most illustrative example occurred during the SHE from 20 to 22 August 2017, although it also appeared in four other instances, most of which were SHEs (Table 2).

The Type 3 configuration is less frequent and involves extreme temperatures in Asturias without the intrusion of warm air at upper atmospheric levels. In such cases, persistent stability affects all atmospheric levels, resulting in stagnant air and localized warming of the air mass in situ. An example of this pattern was observed during the SHE from 2 to 6 August 2018, as well as during the DH from 18 to 21 June 2017. In summary,

the most frequent atmospheric configuration during DHs in Asturias is Type 1, occurring in 72.7% of cases, followed by Type 2 (18,18%) and Type 3 (9,09%). Meanwhile, SHEs align with Type 2 configurations in 50% of cases, Type 1 in 33,3%, and Type 3 in 16,6%. Additionally, the highest 850 hPa temperatures are associated with Type 1 configurations, averaging 24.1 °C, followed by Type 3 at 22 °C, and Type 2 at 21 °C. Table 3 presents the key atmospheric values associated with each DH and SHE that occurred in Asturias, including geopotential height at 500 hPa, temperature at 850 hPa, and surface pressure. The table also indicates the presence or absence of a trough or cut-off low, their positioning, and the corresponding atmospheric configuration type (1, 2, or 3).

The following section presents the synoptic maps corresponding to each case. The situation of the study area in these maps (the region of Asturias) can be observed in the location figure (Figure 4). These maps illustrate the atmospheric configuration (geopotential height, temperature, and surface pressure) across Europe during each of the extreme heat episodes (DHs and SHEs) recorded in the study period. The arrows in the maps indicate, in each case, the direction of the air masses (Figures 5–21).

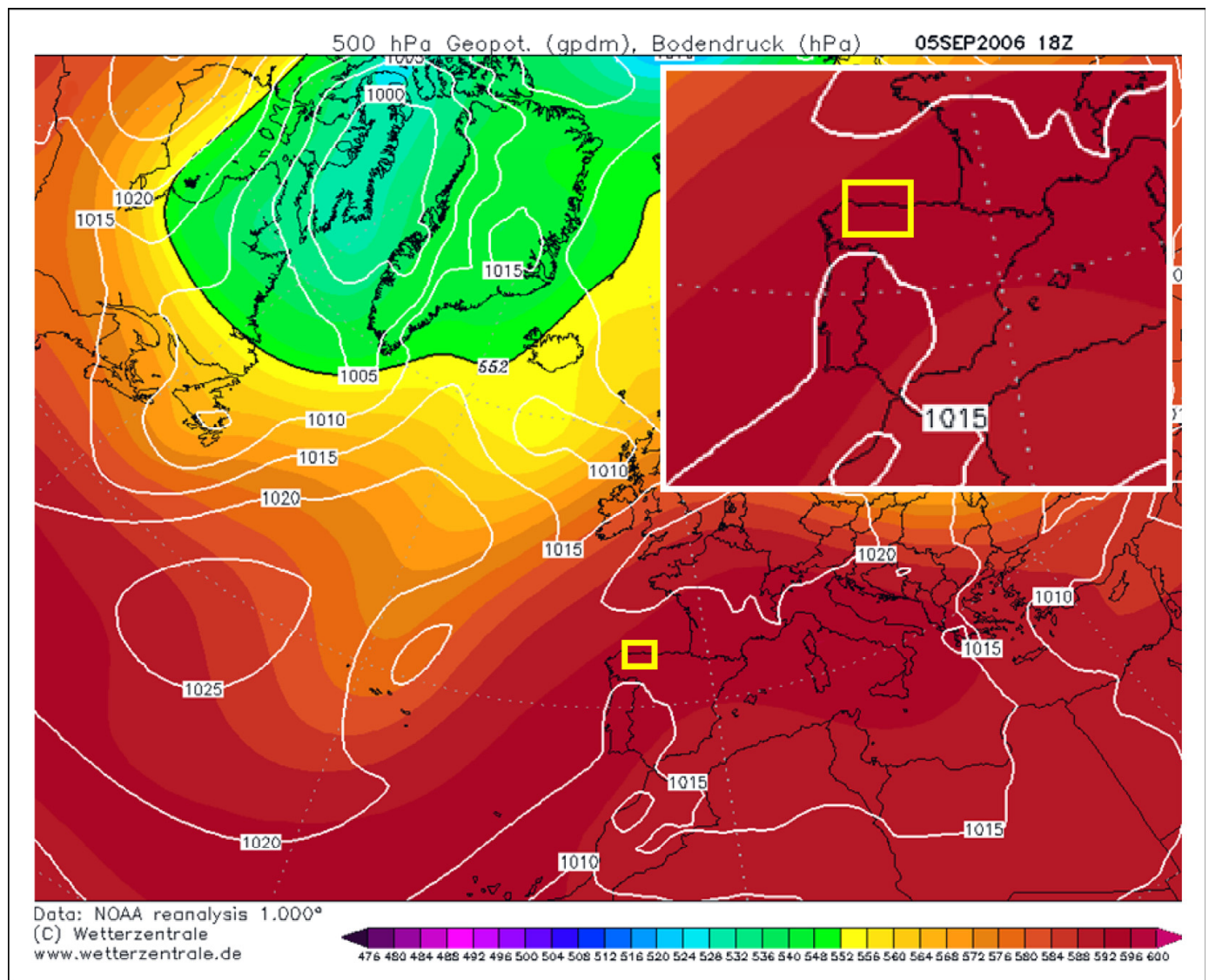


**Figure 4.** The location of the Iberian Peninsula and the region of Asturias (study area) in Europe. Source: Modified from Wetterzentrale.

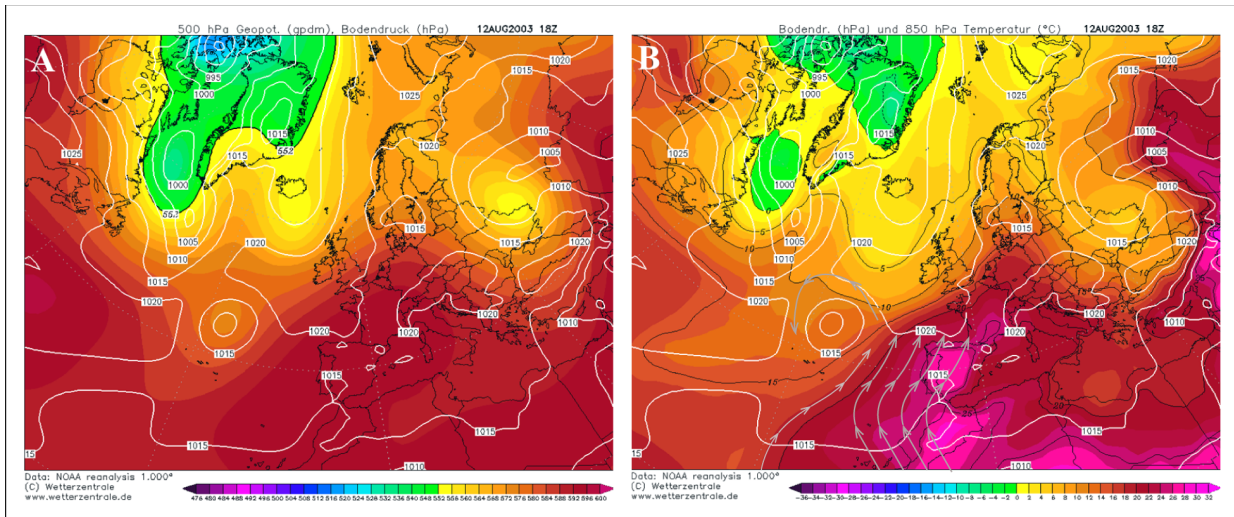


**Figure 5.** Atmospheric configuration during August 2003 DH (12 August). (A) Geopotential map at 500 hPa; (B) temperature map at 850 hPa. Source: Modified from Wetterzentrale.

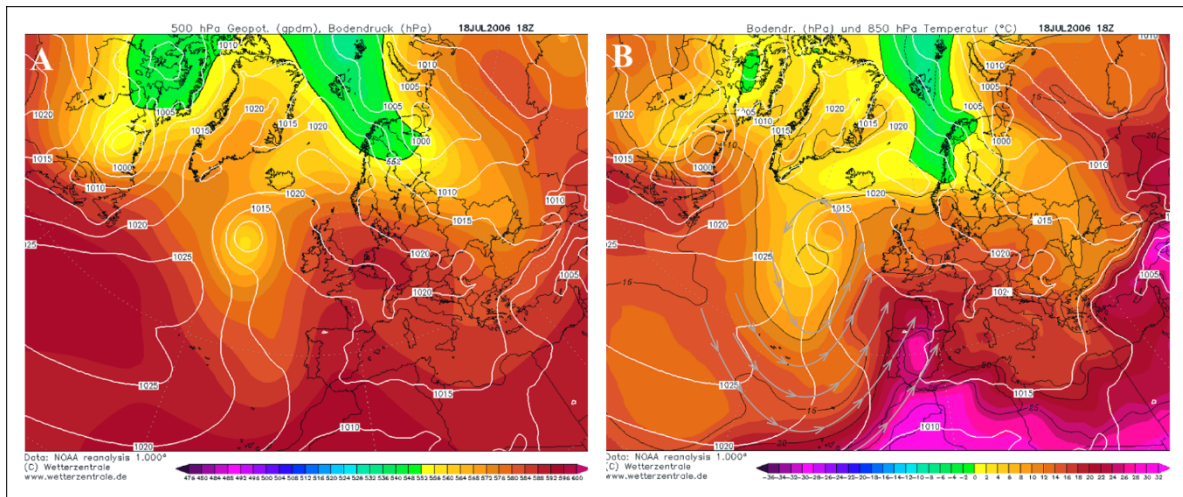


**Figure 6.** Atmospheric configuration during July 2006 SHE (18 July). (A) Geopotential map at 500 hPa; (B) temperature map at 850 hPa. Source: Modified from Wetterzentrale.

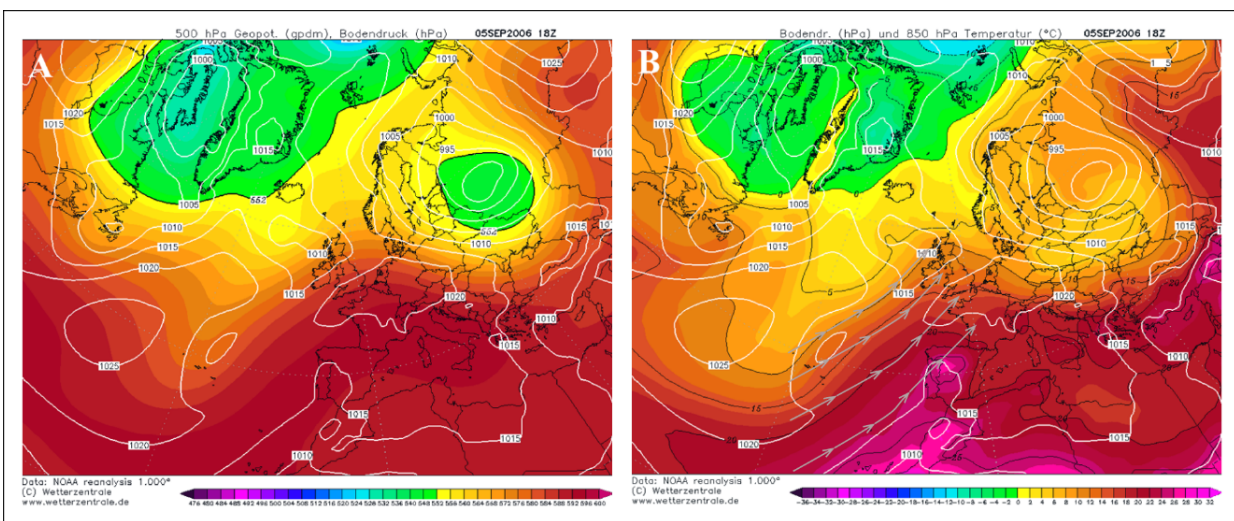


**Figure 7.** Atmospheric configuration during September 2006 DH (5 September). (A) Geopotential map at 500 hPa; (B) temperature map at 850 hPa. Source: Modified from Wetterzentrale.



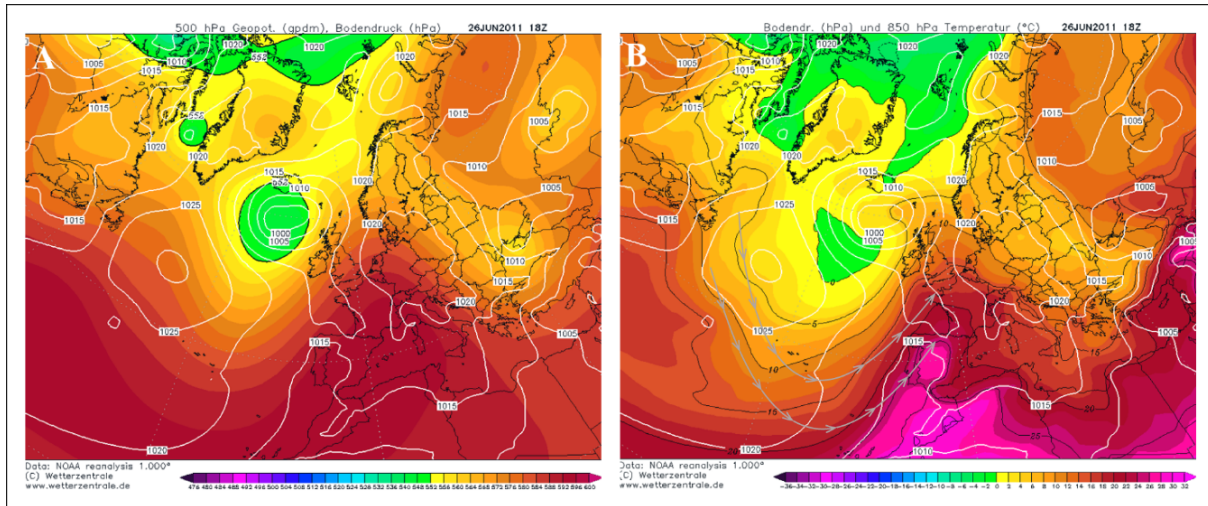


**Figure 8.** Atmospheric configuration during June 2011 SHE (26 June). (A) Geopotential map at 500 hPa; (B) temperature map at 850 hPa. Source: Modified from Wetterzentrale.

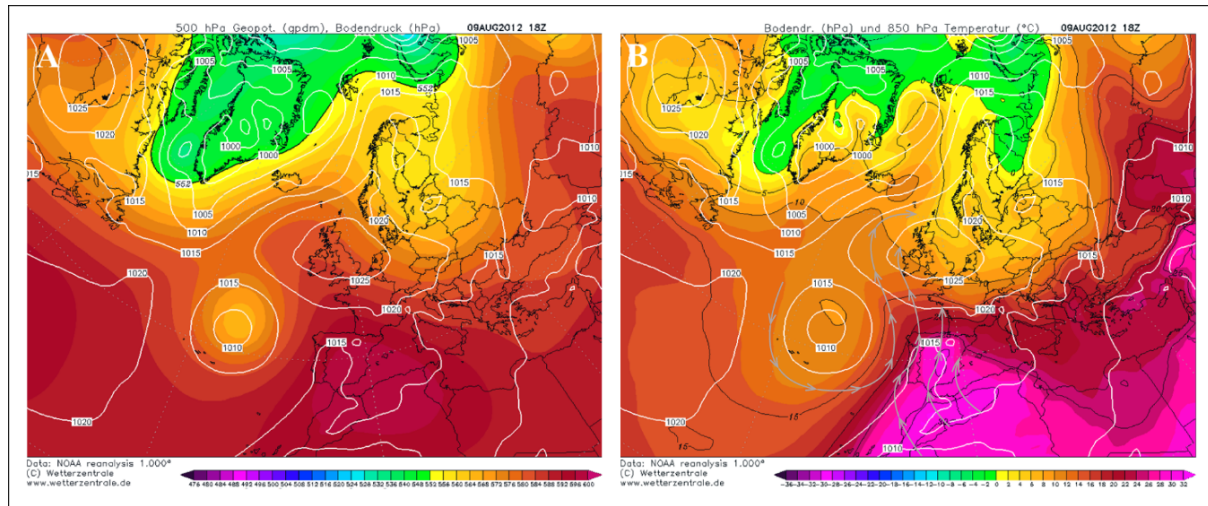


**Figure 9.** Atmospheric configuration during August 2012 DH (9 August). (A) Geopotential map at 500 hPa; (B) temperature map at 850 hPa. Source: Modified from Wetterzentrale.

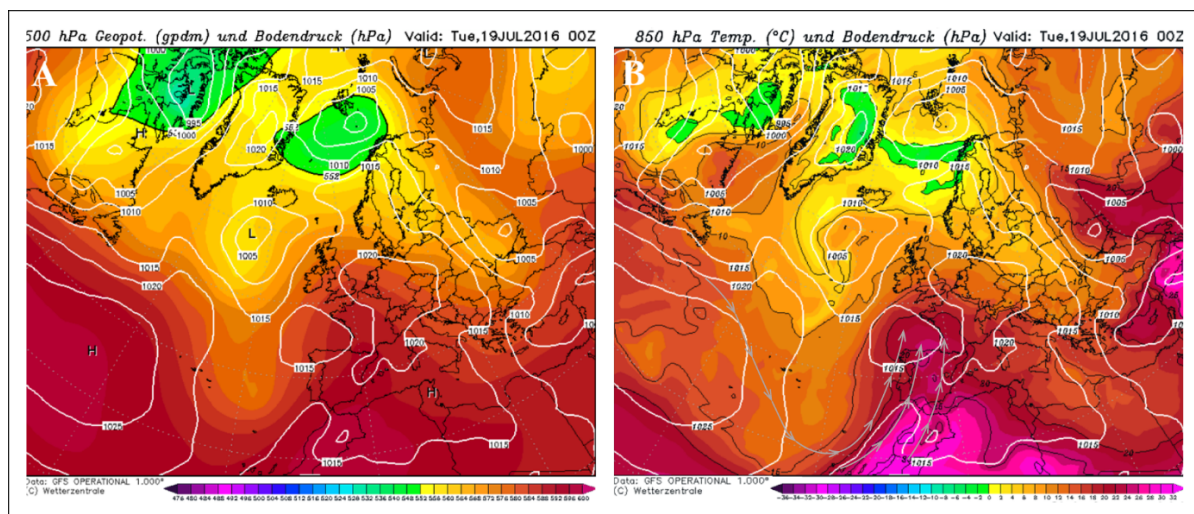


**Figure 10.** Atmospheric configuration during July 2016 DH (19 July). (A) Geopotential map at 500 hPa; (B) temperature map at 850 hPa. Source: Modified from Wetterzentrale.

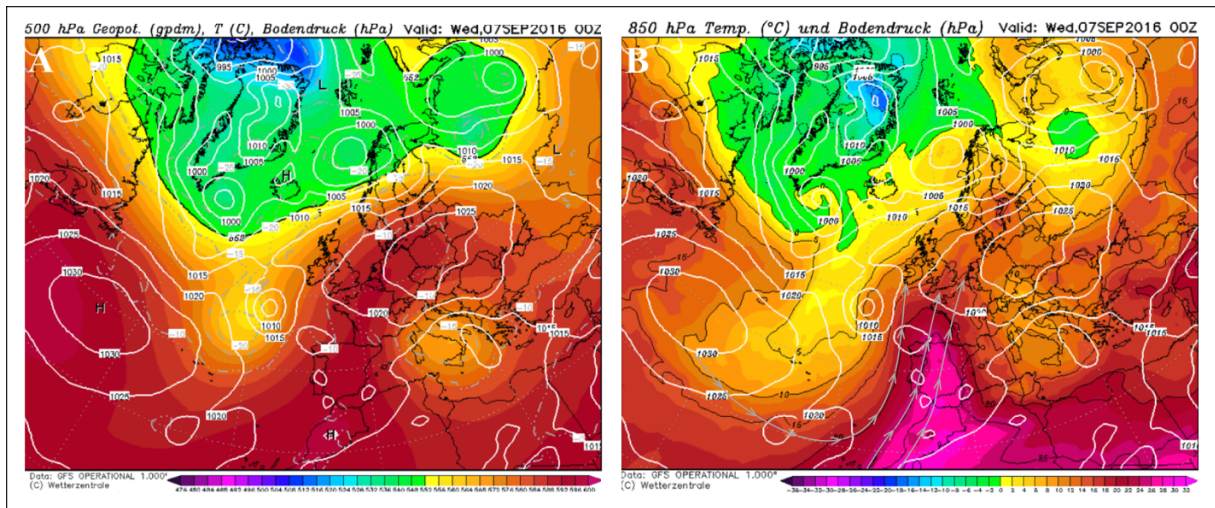


**Figure 11.** Atmospheric configuration during September 2016 DH (7 September). (A) Geopotential map at 500 hPa; (B) temperature map at 850 hPa. Source: Modified from Wetterzentrale.

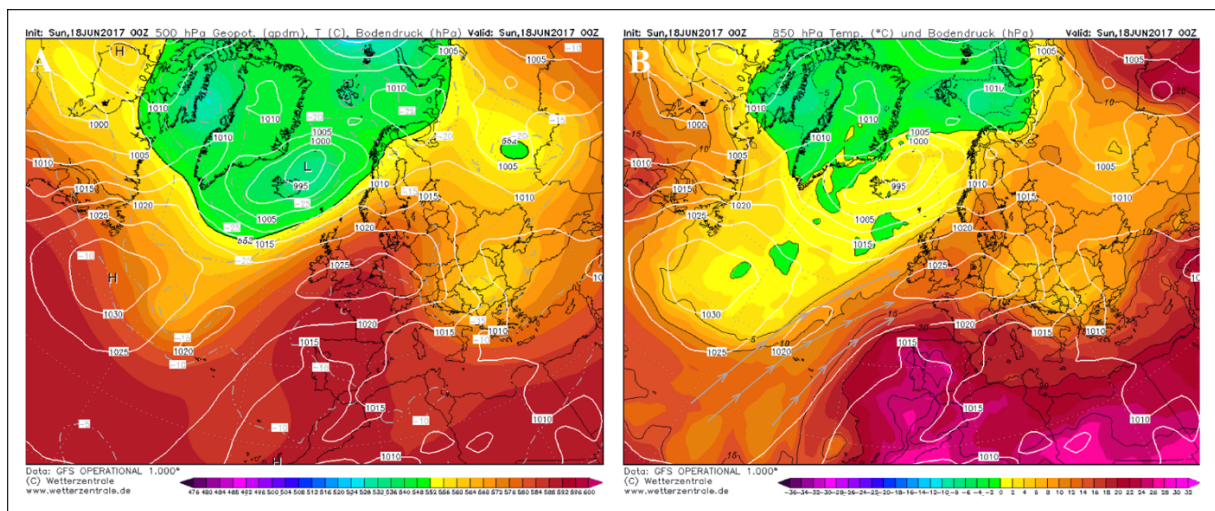


**Figure 12.** Atmospheric configuration during June 2017 DH (18 June). (A) Geopotential map at 500 hPa; (B) temperature map at 850 hPa. Source: Modified from Wetterzentrale.

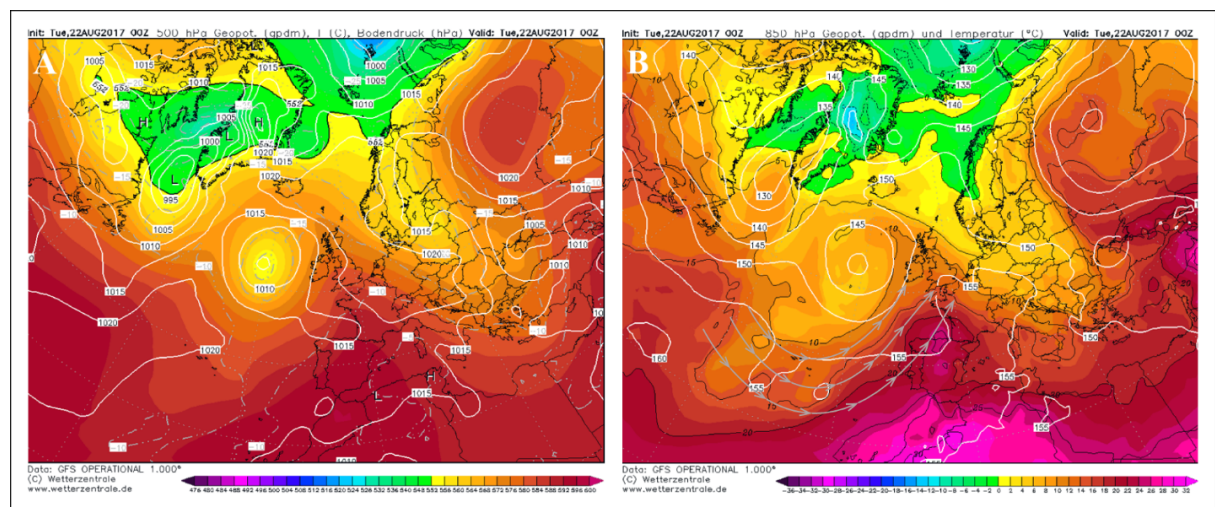


**Figure 13.** Atmospheric configuration during August 2017 DH (22 August). (A) Geopotential map at 500 hPa; (B) temperature map at 850 hPa. Source: Modified from Wetterzentrale.



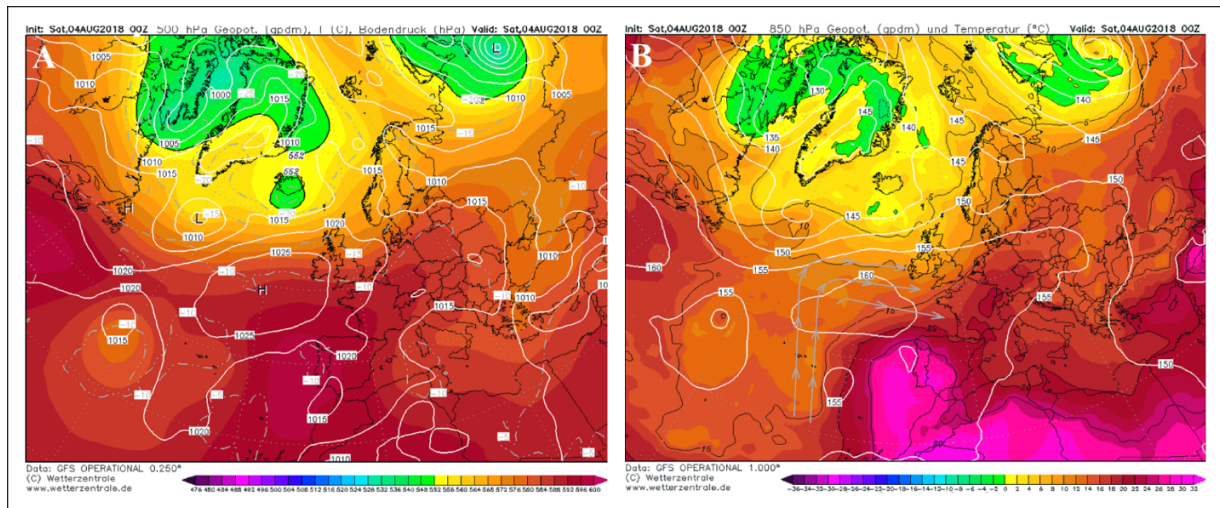


**Figure 14.** Atmospheric configuration during August 2018 SHE (4 August). (A) Geopotential map at 500 hPa; (B) temperature map at 850 hPa. Source: Modified from Wetterzentrale.

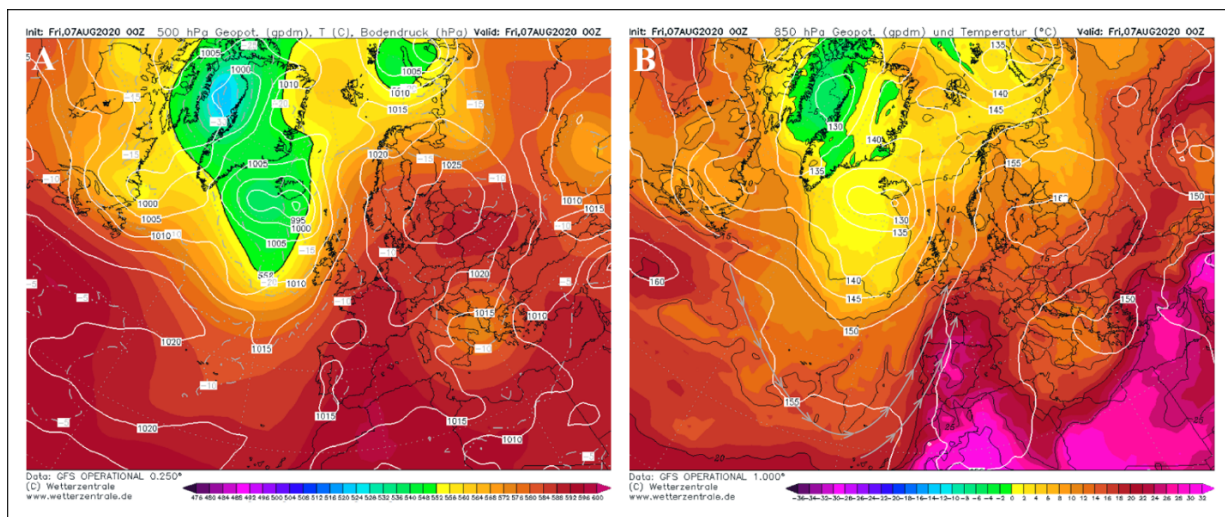


**Figure 15.** Atmospheric configuration during August 2020 SHE (7 August). (A) Geopotential map at 500 hPa; (B) temperature map at 850 hPa. Source: Modified from Wetterzentrale.

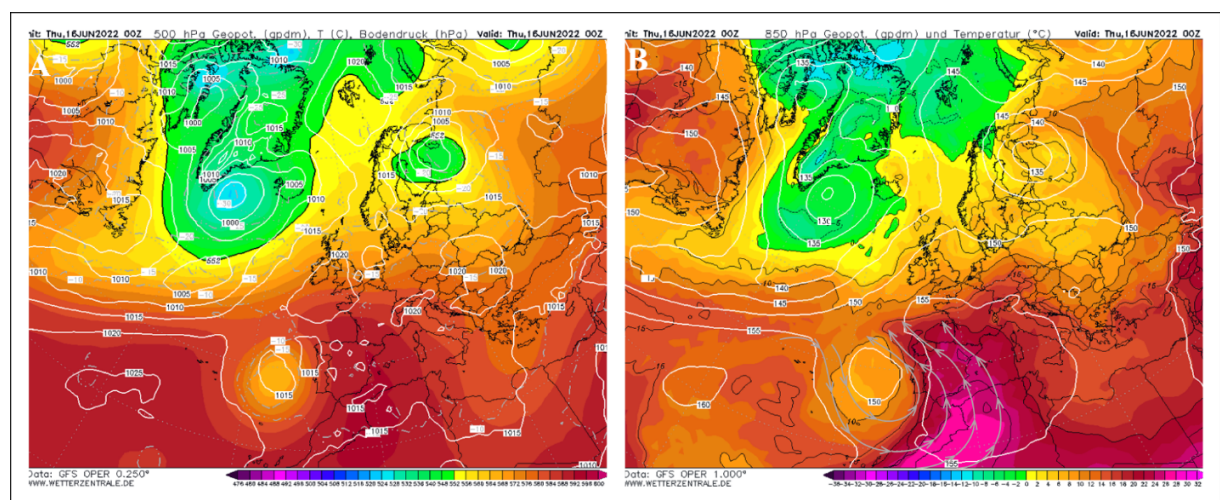


**Figure 16.** Atmospheric configuration during June 2022 DH (16 June). (A) Geopotential map at 500 hPa; (B) temperature map at 850 hPa. Source: Modified from Wetterzentrale.



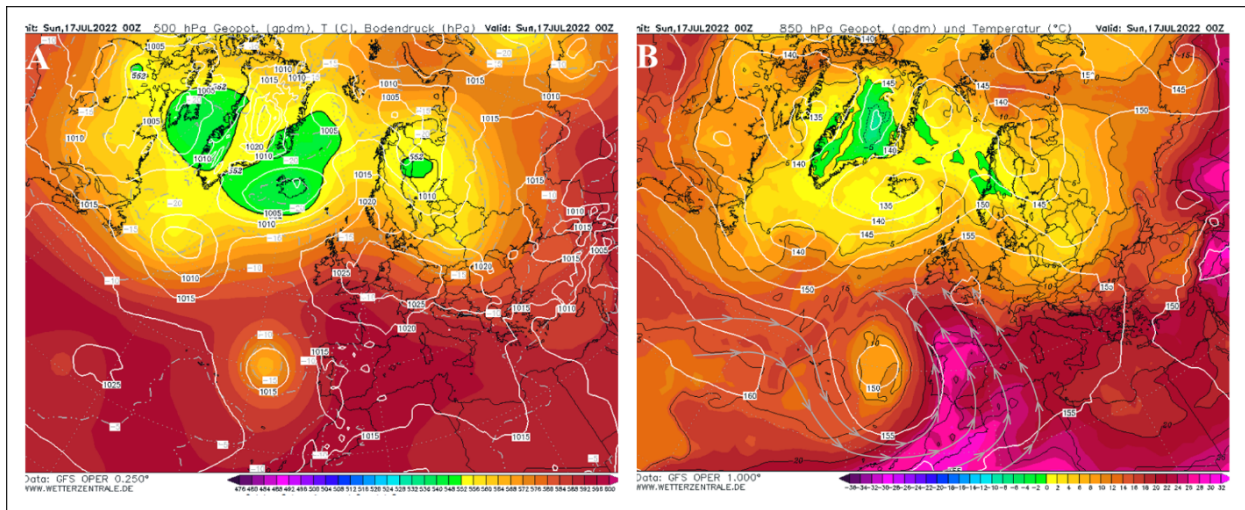


**Figure 17.** Atmospheric configuration during July 2022 DH (17 July). (A) Geopotential map at 500 hPa; (B) temperature map at 850 hPa. Source: Modified from Wetterzentrale.

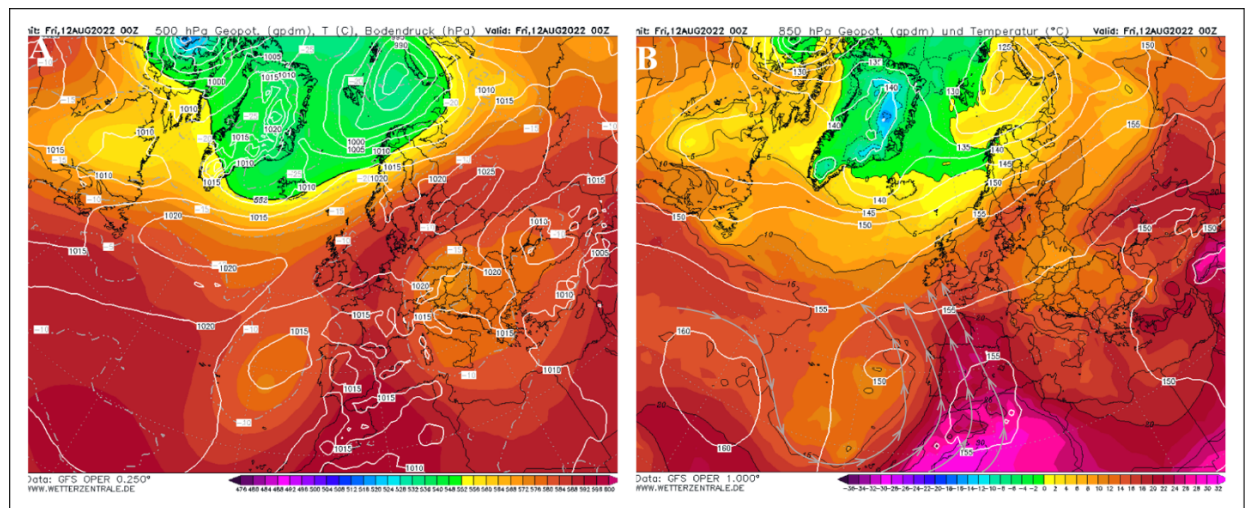


**Figure 18.** Atmospheric configuration during August 2022 SHE (12 August). (A) Geopotential map at 500 hPa; (B) temperature map at 850 hPa. Source: Modified from Wetterzentrale.

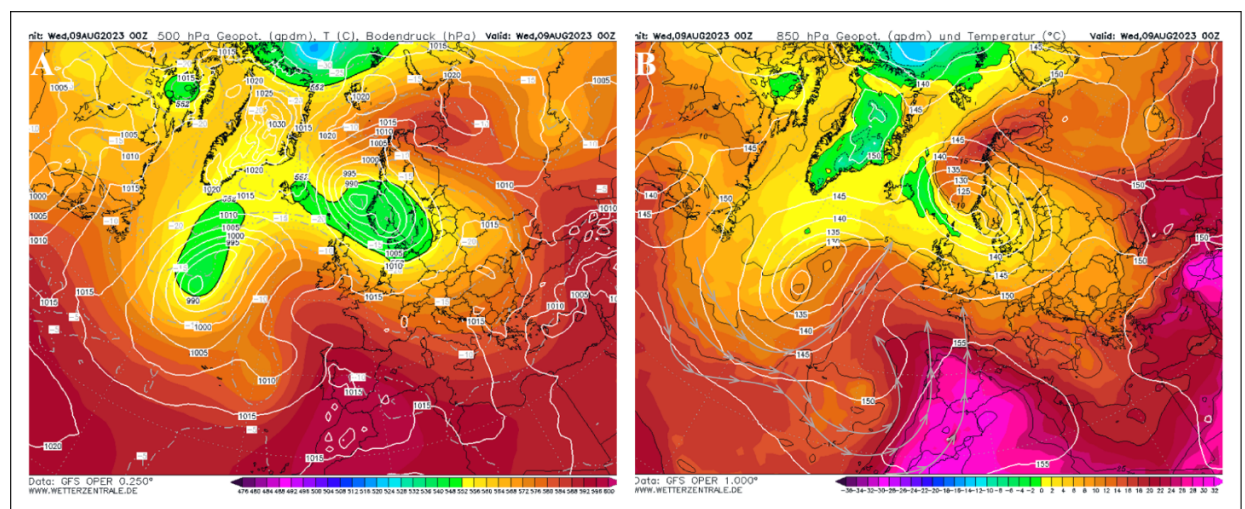


**Figure 19.** Atmospheric configuration during August 2023 DH (9 August). (A) Geopotential map at 500 hPa; (B) temperature map at 850 hPa. Source: Modified from Wetterzentrale.



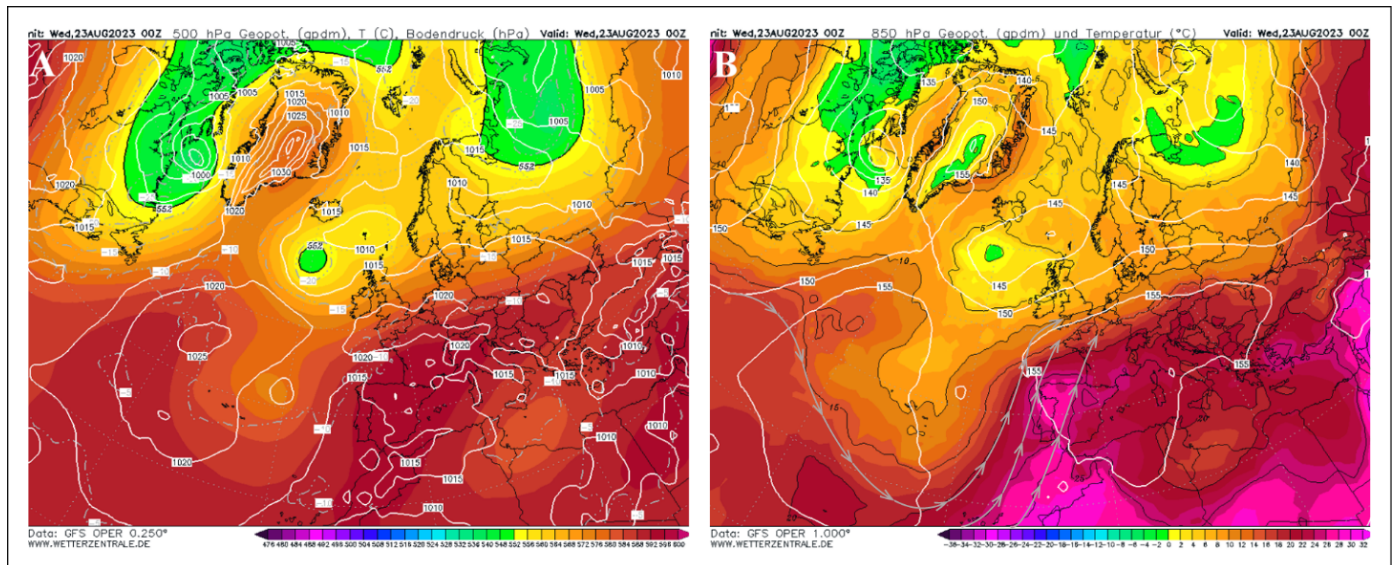


**Figure 20.** Atmospheric configuration during August 2023 DH (23 August). (A) Geopotential map at 500 hPa; (B) temperature map at 850 hPa. Source: Modified from Wetterzentrale.

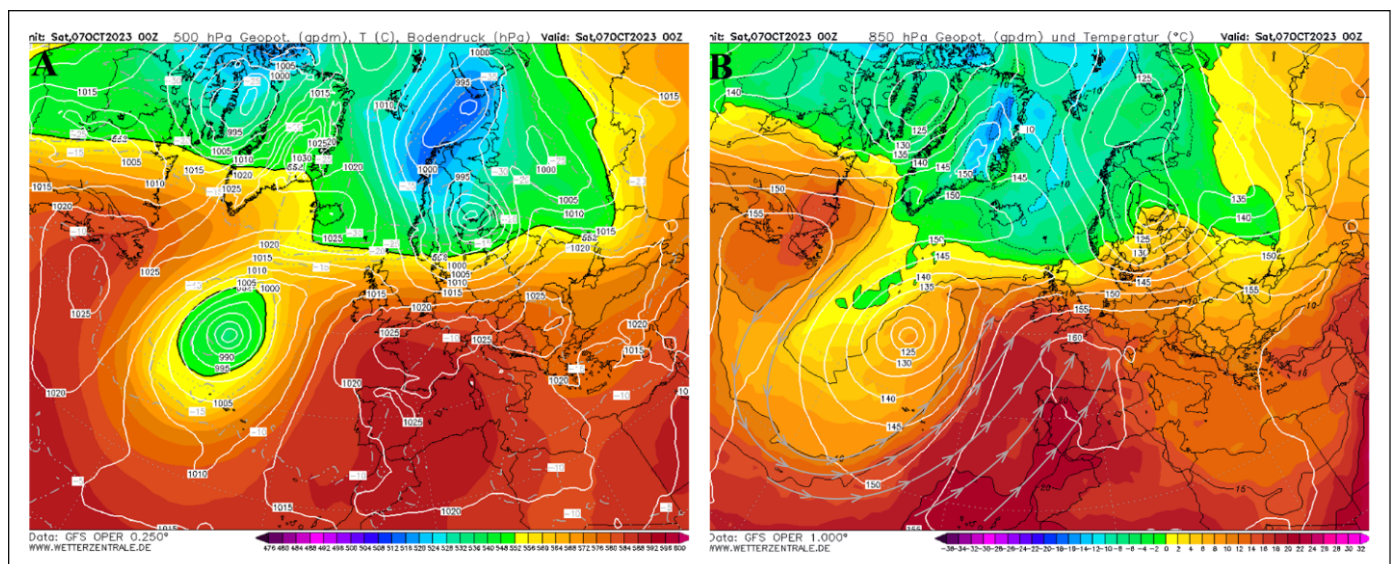


**Figure 21.** Atmospheric configuration during October 2023 SHE (7 October). (A) Geopotential map at 500 hPa; (B) temperature map at 850 hPa. Source: Modified from Wetterzentrale.

### 3.3. Spatial Distribution of Heat Episode Impacts in Asturias

The incidence of heat episodes across the Asturian territory is not homogeneous. Various recurring spatial patterns are observed, which tend to repeat, with the highest temperatures of each episode concentrated in a small number of municipalities (18 out of 78). Asturias is divided into four main sectors, with the coastal and high mountain areas generally not registering the highest temperatures during heat episodes. In contrast, extreme temperature peaks occur in the urban areas of the central region and in the main river valleys, far from the coast.

When selecting the municipalities that have recorded one of the five highest temperatures, in at least four episodes, ten municipalities stand out, located away from the coast. Six of these are in contact with the mountain ranges along the watershed, with greater continuity in the southwestern part of the region, and generally intersected by river valleys (Figure 22). In the southwestern region, those crossed by the Narcea River are particularly

prominent (Tinéu municipality, for example, recorded 11 times), while in the central area, municipalities crossed by the Nalón and Caudal rivers (the latter's tributary) stand out, as well as the valleys of the Huerna and Lena rivers. In the eastern part of Asturias, there is less continuity in the affected municipalities, but they are still related to valleys such as those of the Piloña, Sella, and Cares rivers, with Amieva (nine occasions), Cabrales, and Piloña being particularly notable.

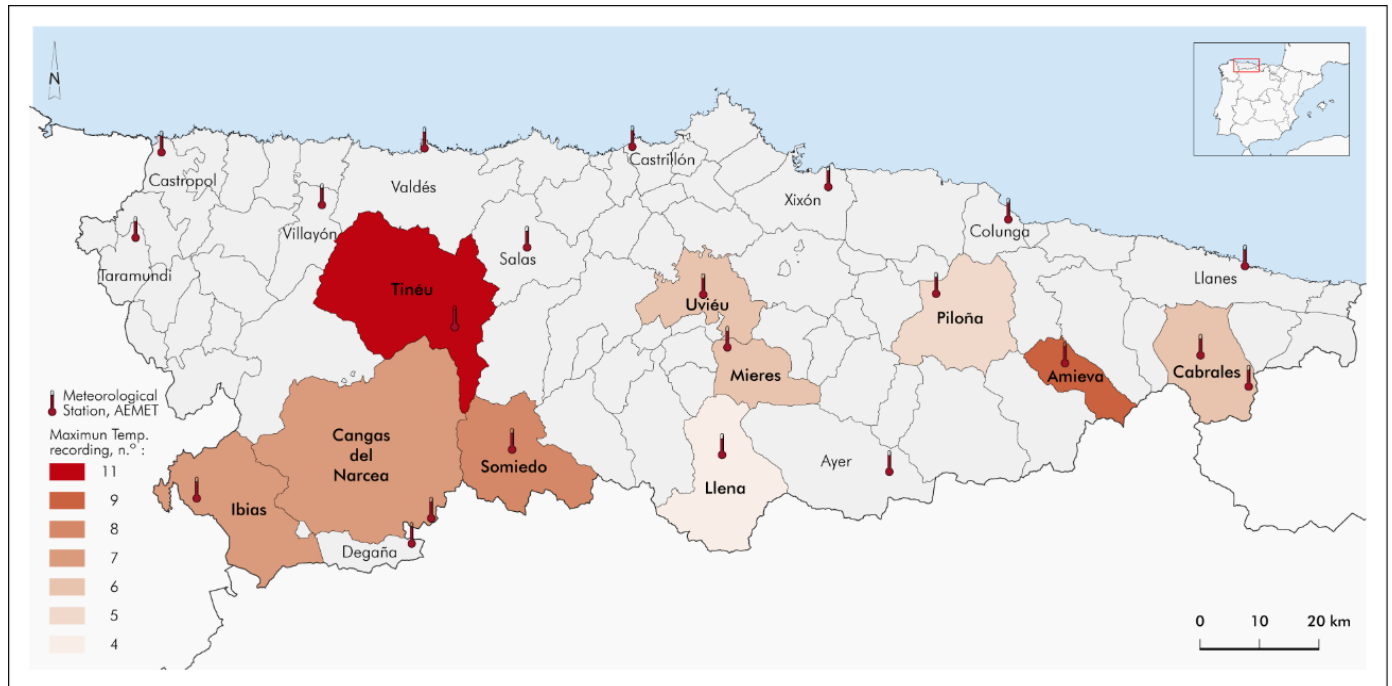


**Figure 22.** Municipalities where one of the five maximum temperature values is reached in at least four extreme heat episodes (DHEs/SHEs), and the location of meteorological stations. Source: Own work.

Meanwhile, municipalities located at higher altitudes do not usually record significant temperature peaks, with exceptions such as Ibias or Somiedo, where the highest temperatures are registered in valley-bottom locations such as Pola de Somiedo or San Antolín de Ibias, similar to Cabrales, which is also at a high altitude but where the highest temperatures occur in the valley bottom of the Cares river. Regarding the urban areas of the central region, Uviéu stands out, with records of maximum temperatures in five episodes.

## 4. Discussion

### 4.1. Extreme Warm Episodes Experienced an Increase in Their Frequency, Duration, and Intensity During the Last Third of the Study Period

#### 4.1.1. Increase in Frequency

The results show an increasing trend in the frequency of extreme heat episodes in Asturias (DHE/SHE), with most of them occurring since 2016 (12 of 17), particularly in the last two years of the series, 2022 and 2023. This increasing trend in recent decades aligns with global observations [19], particularly in Europe [21,23], and across most of Spain [25], especially in the Mediterranean region [26]. Trends observed in Spain since 1950 reflect an increase in the likelihood of extremes: on average, the frequency of DHE has risen by 0.3 per decade, and the probability of experiencing 4–5 events per year has increased eightfold [11].

Studies frame this increase in thermal extremes within the context of the ongoing global climate change process, suggesting that this trend is likely to continue in the future, as highlighted in the latest IPCC report [27]. According to this report, at a global scale, the frequency of heatwaves that currently occur once every 10 years is expected to increase by a factor of 5.6 if the global temperature rise is limited to 2 °C above the pre-industrial average, or by a factor of 9.4 if temperatures rise by 4 °C in the medium to long term (2040 to 2100).

Within the last third of the study period, starting in 2016, we observe years with up to three episodes per year, as seen in 2022 and 2023. This pattern aligns with trends observed globally (e.g., in China and North America), across Europe [28], and particularly in Spain, where the frequency in 2022 and 2023 reached three and four events, respectively [14,25]. There is a clear trend toward increasing frequency, which could lead to episodes that would typically occur once every 10,000 years happening every 4 to 75 years, depending on emission scenarios [9].

#### 4.1.2. Increase in Duration of Episodes

The duration of the episodes generally increased throughout the study period. However, 67.12% of extreme heat days occurred within the time frame starting in 2016. Even within this last third of the period, the increase in duration continues to grow, with the last two years accounting for 38.4% of the total days. This aligns with the average annual increase of 0.9 days per decade recorded between 1950 and 2019, during which the probability of heatwaves lasting more than nine days doubled [11].

#### 4.1.3. Increase in Intensity

Once again, the last third of the period recorded the most significant maximum temperatures and the most notable thermal anomalies, with an average of 35.42 °C during this final third compared to 34.29 °C and 33.45 °C in the second and first thirds of the period, respectively. The episodes of 2022 and 2023 exhibited the highest intensities to date, with average maximum temperatures of 40.03 °C during the DH in July 2022 and 38.86 °C during the DH from August 22 to 24, 2023, also reaching the absolute temperature record in July 2022 (41.4 °C). According to the “Report on the State of the Climate in Spain in 2023” prepared by AEMET [25], the ten warmest years in the historical series since 1961 have been recorded in the 21st century. In Spain, the year 2023 exceeded the average temperature of the reference period 1991–2020 by 1.2 °C, making it the second warmest year in the historical series, only surpassed by 2022, which was 0.3 °C warmer [25].

However, more noteworthy than the increase in the mean temperature anomaly is the observed and projected reduction in the recurrence period of extreme heat events in Spain, as well as their intensity. Climate models indicate that extremes projected for the end of the century are already occurring—they were recorded in 2022 and 2023, much earlier than anticipated—and could recur during this century at least once every 16 years under an intermediate emissions scenario or every 4 years under the worst-case scenario in the current context of climate change [9]. Regarding trends in the thermal intensity of such extremes in Spain, there has been an average increase of 0.1 °C per decade since 1950, doubling the probability of events with anomalies exceeding 1.5 °C [11].

The average summer temperature in Spain in 2022 (24.6 °C) was exceptional, unprecedented in at least 700 years according to paleoclimatic records [14]. The anomaly of 2.1 °C exceeded the mean of the summer maximum temperatures by 4 standard deviations, marking the warmest summer in the Northern Hemisphere in at least two millennia [9]. That same summer was the most exceptional in Asturias in terms of the number of episodes (three), intensity (with temperatures exceeding 40 °C at several stations and reaching



41.4 °C in Mieres), duration (10 days), and its impact on the population, consistent with patterns observed across Spain [14]. This episode triggered, for the first time, level two of the “National Plan of Preventive Actions for High Temperatures”. Nevertheless, there was an increase in heat-related mortality in Asturias of between 2% and 4.5%, with mortality peaks, attributable to extreme heat according to mathematical models from the Carlos III Health Institute, coinciding with the hottest days of the summer [29]. This indicates that, despite the greater climate awareness observed across Spanish society [30] and the integrated early warning systems developed in Europe (Meteoalarm), Asia and Africa (RIMES), and Central America (SAT) [31], deaths and serious health consequences continue to occur. In fact, approximately 60,000 deaths in Europe were linked to extreme heat during the summer of 2022 [9].

#### 4.1.4. The Heatwave in August 2003, an Exception to the Increasing Trend Observed During the Study Period

Despite the increased frequency and intensity of warm episodes in Asturias since 2016, the summer of 2003 continues to stand out as an exception, being the longest heatwave recorded in Asturias to date (11 days). This coincides with observations throughout Spain and Europe. Using an index that combines duration, intensity, and spatial extent, the 2003 heatwave ranks first among all analyzed since 1950 in Spain [11] and had catastrophic effects across Europe, causing over 70,000 deaths [32].

#### 4.2. The Period Covered by Extreme Warm Episodes Within the Year Is Becoming Increasingly Longer

The highest concentration of events occurred between July 15 and August, when temperatures are at their highest in Spain. Thus, 39 of the 73 days with extreme heat episodes took place during this period of the year. This is due to the latitudinal position, which involves greater solar radiation at this time, as well as higher sea temperatures. In fact, during this period, some absolute thermal records were reached in Asturias (not coinciding with any detected extreme heat episode), such as 42 °C on 31 July 2013, at the Amieva-Camporriondi station in the eastern part of the region, and 41.4 °C in Mieres during the July 2022 DH.

In recent decades, a global increase in sea surface temperature has been observed (ranging between 0.68 and 1.01 °C), with a trend indicating that this warming will continue and intensify in the coming years across all seas and oceans worldwide [27], favoring the occurrence heatwaves. In fact, the average surface temperature of the Mediterranean Sea reached a record 28.1 °C in July 2023, with an average anomaly of 1.5 °C compared to the early 1980s [26]. The rise in sea surface temperature can limit the effect of cooling breezes, which require thermal differences between the sea and the land of 3 to 6 °C to function effectively [33]. During the extreme heat episode of August 2018, the water temperature of the Cantabrian Sea in Asturias exceeded 24 °C for the first time, marking a clear trend of warming sea surface temperatures in Spain and the Cantabrian Sea (with 95% confidence) over recent decades [25].

Another important factor contributing to the higher occurrence of thermal extremes in August is the atmospheric circulation during this period. It is likely that the meridional circulation of the jet stream could result in troughs or a cut-off low, responsible for warm air advections over the Iberian Peninsula [34]. A clear example of such persistent atmospheric conditions occurred during the summer of 2022 [14], leading to three extreme heat episodes in Asturias.

However, although this greater concentration of events during July and August has remained largely unchanged over the past 20 years, there is emerging evidence that both DHs and SHEs have progressively shifted toward the early and late periods of the astronomical summer. In 2017, they occurred outside of this season for the first time, a pattern that, while not

statistically significant due to the small sample size, has since repeated twice (2022 and 2023), suggesting a potential trend worth further investigation. This aligns with trends observed in Spain since 1950, where the occurrence period of heatwaves has advanced by 3.8 days per decade while their conclusion has been delayed by 0.5 days per decade [11]. In October 2023, a very late SHE occurred in autumn, which could potentially be attributed to a combination of two factors: a persistently stable atmospheric situation typical of summer [14] and higher-than-usual sea surface temperatures in the Cantabrian Sea, which remained above 20 °C until November, with positive anomalies ranging from +1 to +1.5 °C [25]. While this specific event may be anomalous within the current dataset, it is consistent with the exceptionally warm start to autumn 2023 on a global scale, occurring within a climate change context where events like this are expected to become more frequent, and could not be explained by natural climate variability alone [35].

In summary, while the sample size limits definitive conclusions, there is some evidence suggesting that the temporal range of these extreme heat episodes may have progressively expanded in Asturias, with some events occurring during spring and autumn in the second half of the study period (years 2017, 2022, and 2023). This phenomenon is related to the lengthening of summer observed in Asturias, specifically at the Uviéu station, due to both an extension into autumn and, particularly, an earlier onset in spring [36]. This observation, although preliminary, aligns with the global trend of warm extremes occurring more frequently outside of summer [27], supported by recent studies, such as the April 2023 heat episode in Southern Europe [37], which occurred before summer, like the October 2023 SHE in Asturias, which took place during autumn and may represent part of this broader pattern.

#### *4.3. Three Key Atmospheric Patterns Have Been Identified*

##### *4.3.1. Continental Tropical Warm Advections Originating from Africa Are Responsible for Most of the Warm Episodes That Occurred in Asturias*

Three atmospheric patterns have been identified as responsible for extreme heat episodes in Asturias. Type 3 conditions occur in all cases, characterized by atmospheric stability at all levels, with minimal pressure gradients at the surface. This persistent stability facilitates in situ non-adiabatic heating of the air mass itself through sensible heat transfer in contact with the surface [38]. However, in 15 of the 17 warm episodes, the persistent stability (Type 3) is accompanied by warm air advection at mid- and upper atmospheric levels over the Iberian Peninsula, resulting in a Type 1 or 2 configuration depending on the origin of the air mass, which in turn depends on the prevailing upper-level wind components over Spain.

Type 1 is the most frequent situation (10 out of 17 episodes) and accounts for 72.7% of DH events. It involves the advection of a warm air mass of a continental tropical (Tc) origin at 850 hPa from Africa, with isotherms exceeding 20 °C covering the Cantabrian region. This warm air mass is typically driven by southerly winds at high altitudes due to the presence of a trough or a cut-off low in the Atlantic at 500 hPa. The clearest example of this occurred between 9 and 18 July 2022. The other, less frequent situation (5 out of 17 episodes), classified as Type 2, arises from the advection of a warm maritime tropical (Tm) air mass from the Atlantic, driven by southwesterly winds at high altitudes due to the relative position of a ridge over the Iberian Peninsula at 500 hPa and a trough in the Atlantic between the British Isles and the Azores. This situation was clearly observed between 20 and 22 August 2017.

##### *4.3.2. Commonalities and Differences Between the Three Identified Pattern Types*

With the aim of better observing the similarities and differences among the main atmospheric patterns identified, Figure 23 presents a comparison of three representative examples of each type of situation responsible for extreme heat episodes in Asturias.

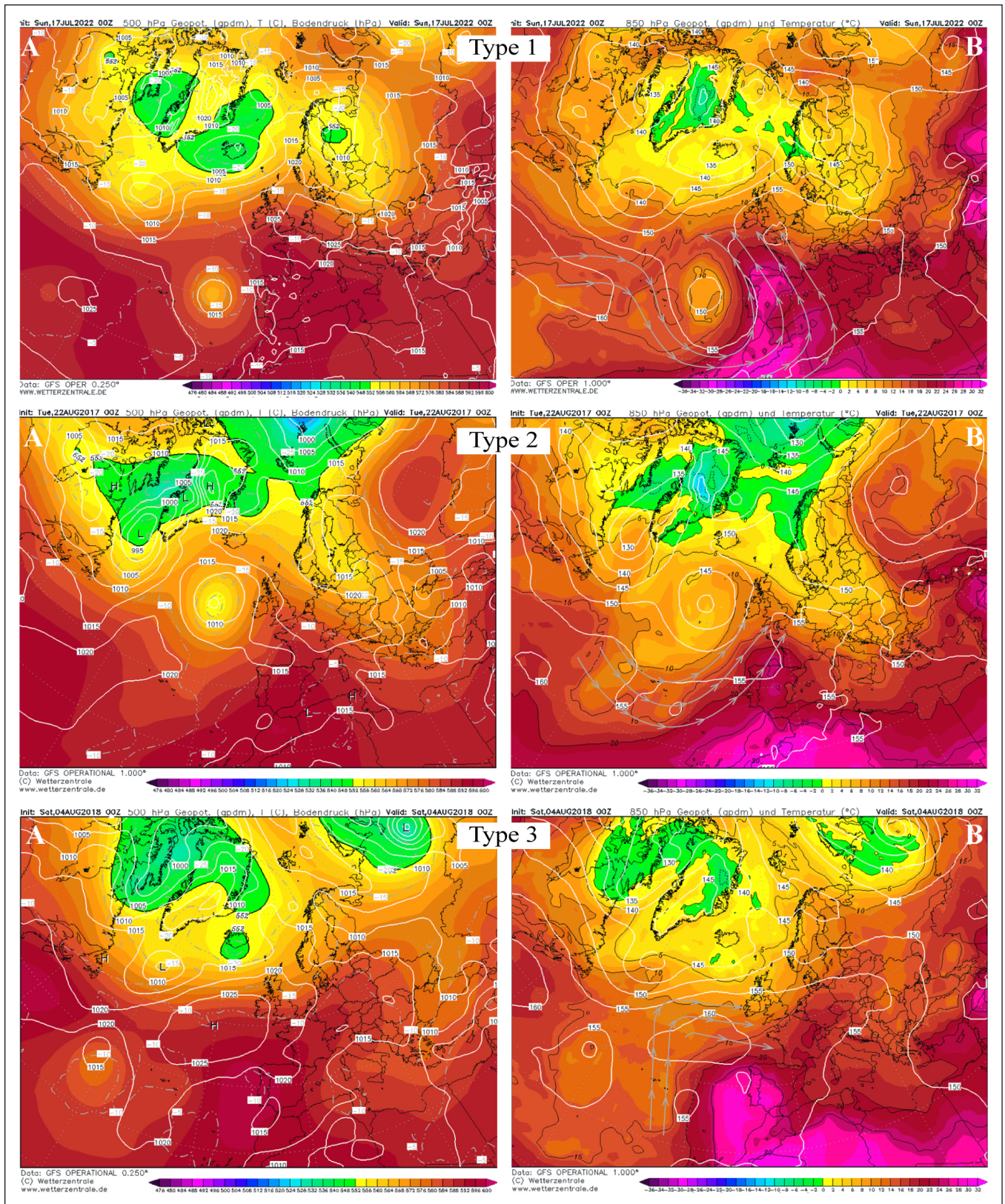


**Figure 23.** Comparison among the three main atmospheric conditions that lead to extreme heat episodes in Asturias. Source: Modified from Wetterzentrale.

There is a common characteristic shared by the three types of atmospheric situations. The primary similarity is the clear predominance of atmospheric stability over the Iberian Peninsula at all levels of the atmosphere. This stability is evident at the surface, with the



presence of the Azores High, and at mid- and upper levels of the atmosphere, where a ridge is located. In all three cases, this stability results in a weak barometric gradient at the surface, which inhibits air movement and leads to its warming.

However, significant differences exist between Type 1 and Type 2 situations on one hand, and Type 3 situations on the other. In Type 3 situations, extreme heat arises solely from atmospheric stability, which causes air masses to warm due to a lack of ventilation. In contrast, both Type 1 and Type 2 situations involve an additional mechanism: the advection of a warm air mass of a tropical origin. Therefore, Type 1 and Type 2 situations share atmospheric stability and warm advection caused by the presence of a trough or a cut-off low over the Atlantic. The relative position of these features to the ridge drives the advection of warm air masses over the Iberian Peninsula, a process absent in Type 3 situations.

The key difference between Type 1 and Type 2 situations lies in the relative position of the Atlantic trough with respect to the ridge over the peninsula. This positioning determines the predominant wind component at mid- and upper atmospheric levels and, consequently, the continental or maritime nature of the warm air mass advection. Specifically, during Type 1 situations, southerly winds prevail at mid- and upper levels, driving a tropical continental air mass from the African continent with minimal maritime influence over the Iberian Peninsula. Conversely, in Type 2 situations, southwesterly winds dominate at higher levels, generating warm advection over the peninsula. However, in this case, the advected air mass is tropical maritime in nature, traversing the Atlantic and resulting in less extreme temperatures compared to the continental advectations of Type 1.

#### 4.3.3. Variations in Atmospheric Circulation and Their Potential Influence on the Occurrence of Warm Extremes

Type 1 and Type 2 situations are generated by the meridional circulation of the jet stream. This meridional circulation can lead to episodes of summer rains and storms or warm advectations over the Iberian Peninsula, depending on the relative position of ridges and troughs [34]. In both types of situations, at the 500 hPa level, a ridge is present over Spain, while a trough or cut-off is located over the Atlantic, causing the advection of a warm air mass over the peninsula. The difference between the two lies in the position and tilt of the trough, which influences the predominant wind component and, consequently, the nature of the warm air advection over the peninsula, which can be continental (Type 1) or maritime (Type 2). The nature of the air mass affects the average temperatures reached at altitude with each configuration, being higher in the case of continental air masses (24.1 °C) compared to maritime ones (21 °C). Therefore, the occurrence of thermal extremes is directly linked to atmospheric circulation and is always associated with positive anomalies in surface pressure, geopotential height at 500 hPa, and temperature at 850 hPa, as demonstrated by other studies on the causes of heatwaves in Europe [39] and specifically over the Iberian Peninsula [40]. In the current context of global change, it is crucial to understand potential changes in atmospheric circulation and their possible impacts on heatwaves over the Iberian Peninsula.

Several recent studies suggest that variations in atmospheric circulation are already occurring, leading to a temperature increase in the Mediterranean region (1.5 °C) that significantly exceeds the global average (1.1 °C). This is attributed to a weakening of the jet stream, which generates greater undulations and increases the likelihood of reaching extreme temperatures by promoting the occurrence of the previously mentioned atmospheric conditions [26]. Similarly, other studies suggest that in the Northern Hemisphere, the amplified warming of Arctic regions leads to a reduced north–south thermal gradient, resulting in a weakening of the jet stream. This reduction in velocity increases the probability of meridional circulation with pronounced undulations [41].

#### 4.3.4. The Exceptional Nature of the Summer of 2022

Among Type 1 situations, the one between 9 and 18 July 2022 stands out due to the exceptional temperatures reached at 850 hPa with the 30 °C isotherm brushing the Cantabrian coast. This occurred due to the persistence of the episode (which enhances the warming of the air mass), the position of a cut-off low that drove southerly winds at mid-to-high levels of the atmosphere, and the very warm nature of the tropical continental air mass, coinciding with the period of the highest solar radiation. In Type 1 configurations, it is precisely the differences in temperature of this air mass originating from Africa that determine the varying intensities of episodes; for instance, the maximum temperature values reached during the June 2022 episodes were lower than those in July 2022, despite very similar atmospheric configurations. In contrast, when compared to Type 2 situations, the differences in temperature observed between episodes are due to the different nature of the air mass, with all cases exhibiting higher temperatures at 850 hPa in Type 1 than in Type 2, as these are continental air masses (Tc).

#### 4.4. The Highest Incidence of Warm Extremes Is Observed in Urban Areas and River Valleys

The intensity of warm episodes is not solely dependent on the atmospheric configurations that trigger them; rather, how air masses interact with the terrain and land use is crucial. This interaction significantly moderates the effects of heatwaves on different areas of the Asturias territory.

First, the contrast between the limited impact of warm episodes on the coast compared to the rest of the Asturian territory stands out. On the coast, there are barely any records of extreme heat due to the influence of marine breezes [33,42] and advection fogs [43], which help cool the environment. Additionally, the stability of the atmosphere typical during a heatwave supports the presence of coastal breezes, as the warming of air in contact with the surface in nearby land areas to the sea generates relative low pressure, prompting air movement from the Cantabrian Sea towards the coast, similar to the Mediterranean [33], thereby intensifying the thermal contrasts with the interior where the breeze does not penetrate. However, studies of this type on the Cantabrian coast, and specifically in Asturias, are lacking to understand its behavior and relationship with heatwaves. Instead, despite no heatwaves being recorded on the Asturian coast, a recent study on the evolution of thermal comfort in coastal areas of Spain [44] reveals that the greatest decrease in thermal comfort in Spain during recent summers has occurred on the eastern coast of Asturias.

On the other hand, there is also a clear contrast between urban and rural areas. The extreme values in the central metropolitan area of Asturias (Avilés, Mieres, Llangréu, Uviéu, Xixón) are especially explained by the urban heat island effect, which causes higher temperatures in cities compared to nearby rural environments. This effect is amplified during heatwaves and is closely related to these phenomena [45]. This effect is due to the different capacity of artificial surfaces to absorb and emit solar radiation compared to green areas, increasing the population's vulnerability in cities [46]. For example, in the case of Barcelona, the urban heat island effect contributes between 2 °C and 7 °C more than in surrounding areas, and it has also increased with climate change [47]. This effect can explain, for example, why Avilés or Xixón are the only coastal observatories that record extreme temperatures. Numerous studies emphasize the importance of this phenomenon globally [48,49], particularly in Spanish cities [50–56]. The latter study analyzes the effect on the city of Zaragoza, concluding that it is more frequent under atmospheric stability conditions, as is the case during heatwave episodes, and at night hours, which is also related to the increase in tropical nights in Spain, particularly in the Mediterranean basin [57], but also on the Atlantic coast and in Galicia [58]. Studies on the Cantabrian region and Asturias are scarce, which would be interesting given that warm nights can be responsible for high



mortality during heatwaves [59]. The increase in tropical nights in Spain, defined as those where the temperature does not drop below 20 °C, is clearly linked to the growing trend of heatwave phenomena [60].

Outside of metropolitan areas, it is observed that the most affected spaces by heat are those situated in river valleys, such as the Narcea in the west and the Cares in the east. Under conditions of atmospheric stability, valley bottoms experience warming in two ways: either due to the lack of ventilation, so that the air mass heats up non-adiabatically by heat transmission from the valley floor, or the warming is increased by the compression of air descending into the valley bottom, known as adiabatic warming [38]. These situations are amplified when a southerly wind blows, common during heatwave episodes of Types 1 and 2, as the wind ascends the southern slopes of the Asturian mountain range, cools, and loses most of its humidity before descending the lee slopes as warm, dry air, raising temperatures in valleys through the “Foehn effect,” which has been widely studied internationally [61,62] and linked to heatwaves in the case of South Korea [63], Japan [64], or Antarctica [65]. This “Foehn effect” in Asturias is especially pronounced in valleys oriented north–south, which better channel these flows, as opposed to those oriented east–west, where this effect is less intense. The meridional orientation of valleys is more apparent in the southwestern and central parts of the region, where the most extreme temperatures are recorded, such as Tinéu in the Narcea Valley. In contrast, in the eastern part of the region, the predominant valley orientation is east–west, and fewer extreme temperatures are recorded, possibly due to the lack of weather stations, for example, in Alto Nalón. Finally, the lack of weather stations is compounded by an informational bias, where the media often pay more attention to more populated (urban) areas [66], making it difficult to draw conclusions in such a complex region like Asturias.

## 5. Conclusions

This study examined the frequency, duration, and intensity of extreme heat episodes in Asturias, an Atlantic region in the NW of Spain, between 2001 and 2023. The research analyzed the evolution of the phenomenon, the atmospheric conditions that cause it, and territorial contrasts. A novel methodology was employed, enabling the detection of a greater number of warm episodes (SHEs) based on local press sources, in addition to the officially declared heatwaves (DHs).

The observations indicate a consistent increase throughout the study period, particularly during the last 8 years. The frequency, duration, and intensity of episodes significantly rose during this latter third starting in 2016, with the sole previous exception of the summer of 2003. A particularly notable recent increase is reflected in the exceptional nature of the last two years of the studied period (2022 and 2023). It has also been observed that the temporal duration of warm extremes throughout the year is becoming increasingly extended. Although most episodes occurred between mid-July and mid-August, during the last third of the study period, three episodes were recorded outside the astronomical summer: two in spring and one in autumn (October 2023). While these observations are based on a limited dataset and should be interpreted with caution, they suggest a potential expansion of the temporal window for warm extremes. Both developments are not an isolated occurrence; rather, they fit with patterns observed across Southern Europe and global observations.

Regarding atmospheric patterns, three key configurations have been identified as responsible for warm episodes in the northwest of Spain. Type 1 is the most frequent (10 out of 17) and is associated with the advection of a continental tropical air mass from Africa (Tc), driven by southerly winds. Type 2, which occurs on five occasions, corresponds to the advection of a maritime tropical air mass (Tm) due to southwesterly winds. Type 1 situations are associated with warmer temperatures at 850 hPa than Type 2 (24.1 °C vs. 21 °C), due to the different nature of the air masses, with continental masses reaching

higher temperatures. Finally, Type 3 is associated with persistent atmospheric stability, with an absence of winds that favors the warming of air in contact with the surface, and it occurred only twice. As the global energy balance destabilizes in the context of climate change, variations in large-scale atmospheric circulation may lead to changes in the usual patterns in the study region, increasing the frequency of conditions conducive to warm advections and, consequently, the occurrence of extreme heat episodes.

On the other hand, there are notable differences across the Asturian territory regarding the incidence of heat episodes, with the interaction between atmospheric configuration and topography and land use playing a key role. Coastal areas have so far remained largely unaffected by most heat episodes due to the mitigating effects of sea breezes and advection fog. However, the recent warming of the sea surface may reduce this effect, although specific studies on this phenomenon in the Cantabrian area are lacking. Urban areas in Asturias have recorded the highest temperatures during heat episodes due to the urban heat island effect, which has been extensively documented in Spanish and global cities. In addition to urban areas, river valleys have also shown significant temperature increases. This is attributed to greater air warming in valley bottoms through two mechanisms: sensible heat transfer from the ground in conditions of stagnant air, and adiabatic warming due to the compression of air descending along the slopes. This warming is further intensified by the Foehn effect during Type 1 and Type 2 atmospheric configurations with southerly winds. These winds ascend the southern slopes of the Asturian Massif, losing moisture and temperature, and descend as warm, dry air. This effect is particularly pronounced in north–south-oriented valleys, such as the Narcea Valley, which experiences the highest temperatures during heat episodes.

This study aims to shed light on recent changes in an oceanic climate area in Southern Europe, where heat extremes have traditionally been absent: observed patterns are becoming worrisome in this Atlantic sector, given the recent increase in the frequency, duration, and intensity of heat extremes, consistent with regional and global trends in the current context of climate change. Therefore, this study should serve as a starting point for the development of further research on this issue in Atlantic areas, with the aim of contributing, as much as possible, to mitigation and adaptation efforts.

**Author Contributions:** Conceptualization, methodology, and writing—original draft, L.P.-G. and C.G.-H.; investigation and data curation, L.P.-G.; writing—review and editing, L.P.-G., C.G.-H. and J.R.-F.; formal analysis and supervision, C.G.-H. and J.R.-F. All authors have read and agreed to the published version of the manuscript.

**Funding:** This research was funded by the PARANTAR project (PID2020-115269GB-I00; Ministry of Science, Innovation and Universities of the Government of Spain).

**Data Availability Statement:** The data presented in this study are available on request from the corresponding author. The data are not publicly available due to size and institutional restrictions.

**Conflicts of Interest:** The authors declare no conflicts of interest.

## References

1. Conlon, K.C.; Mallen, E.; Gronlund, C.J.; Berrocal, V.J.; Larsen, L.; O'Neill, M.S. Mapping human vulnerability to extreme heat: A critical assessment of heat vulnerability indices created using principal components analysis. *Environ. Health Perspect.* **2020**, *128*, 97001. [[CrossRef](#)]
2. Licker, R.; Dahl, K.; Abatzoglou, J.T. Quantifying the impact of future extreme heat on the outdoor work sector in the United States. *Elem. Sci. Anth.* **2022**, *10*, 00048. [[CrossRef](#)]
3. Gamero-Salinas, J.; López-Hernández, D.; González-Martínez, P.; Arriazu-Ramos, A.; Monge-Barrio, A.; Sánchez-Ostiz, A. Exploring indoor thermal comfort and its causes and consequences amid heatwaves in a Southern European city—An unsupervised learning approach. *Build. Environ.* **2024**, *265*, 111986. [[CrossRef](#)]

4. Tong, S.; Prior, J.; McGregor, G.; Shi, X.; Kinney, P. Urban heat: An increasing threat to global health. *BMJ* **2021**, *375*, 2467. [[CrossRef](#)] [[PubMed](#)]
5. Perkins-Kirkpatrick, S.E.; Lewis, S.C. Increasing trends in regional heatwaves. *Nat. Commun.* **2020**, *11*, 3357. [[CrossRef](#)]
6. Ebi, K.L.; Capon, A.; Berry, P.; Broderick, C.; de Dear, R.; Havenith, G.; Jay, O. Hot weather and heat extremes: Health risks. *Lancet* **2021**, *398*, 698–708. [[CrossRef](#)] [[PubMed](#)]
7. González-Trujillo, J.D.; Román-Cuesta, R.M.; Muñoz-Castillo, A.I.; Amaral, C.H.; Araújo, M.B. Multiple dimensions of extreme weather events and their impacts on biodiversity. *Clim. Chang.* **2023**, *176*, 155. [[CrossRef](#)]
8. Morabito, M.; Crisci, A.; Messeri, A.; Messeri, G.; Betti, G.; Orlandini, S.; Maracchi, G. Increasing heatwave hazards in the southeastern European Union capitals. *Atmosphere* **2017**, *8*, 115. [[CrossRef](#)]
9. Tejedor, E.; Benito, G.; Serrano-Notivol, R.; González-Rouco, F.; Esper, J.; Büntgen, U. Recent heatwaves as a prelude to climate extremes in the western Mediterranean region. *Npj Clim. Atmos. Sci.* **2024**, *7*, 218. [[CrossRef](#)]
10. Adélaïde, L.; Chanel, O.; Pascal, M. Health effects from heat waves in France: An economic evaluation. *Eur. J. Health Econ.* **2022**, *23*, 119–131. [[CrossRef](#)]
11. Paredes-Fortuny, L.; Khodayar, S. Understanding the Magnification of Heatwaves over Spain: Relevant changes in the most extreme events. *Weather Clim. Extrem.* **2023**, *42*, 100631. [[CrossRef](#)]
12. Guo, Y.; Gasparrini, A.; Li, S.; Sera, F.; Vicedo-Cabrera, A.M.; de Sousa Zanotti Stagliorio Coelho, M.; Tong, S. Quantifying excess deaths related to heatwaves under climate change scenarios: A multicountry time series modelling study. *PLoS Med.* **2018**, *15*, e1002629. [[CrossRef](#)]
13. Domingo, D.; Vicente-Serrano, S.M.; Gómez, C.; Olano, J.M.; Sangüesa-Barreda, G. Summer heat waves could counterbalance the increasing incidence of pine processionary due to warmer winters in Mediterranean pine forests. *For. Ecol. Manag.* **2024**, *555*, 121695. [[CrossRef](#)]
14. Serrano-Notivol, R.; Tejedor, E.; Sarricolea, P.; Meseguer-Ruiz, O.; de Luis, M.; Saz, M.Á.; Longares, L.A.; Olcina-Cantos, J. Unprecedented warmth: A look at Spain's exceptional summer of 2022. *Atmos. Res.* **2023**, *293*, 106931. [[CrossRef](#)]
15. Vargas-Amelin, E.; Pindado, P. The challenge of climate change in Spain: Water resources, agriculture and land. *J. Hydrol.* **2014**, *518*, 243–249. [[CrossRef](#)]
16. Olcina-Cantos, J.; Vera-Rebollo, J.F. Cambio climático y política turística en España: Diagnóstico del litoral mediterráneo español. *Cuad. De Tur.* **2016**, *38*, 327–363. [[CrossRef](#)]
17. Sánchez-Sánchez, M.D.; De Pablos-Heredero, C.; Botella, J.L.M. Impact of Heat Waves on the Redistribution of Tourist Flows: The Case of Spain. *Preprints* **2024**. [[CrossRef](#)]
18. Díaz, J.; Sáez, M.; Carmona, R.; Mirón, I.; Barceló, M.A.; Luna, M.Y.; Linares, C. Mortality attributable to high temperatures over the 2021–2050 and 2051–2100 time horizons in Spain: Adaptation and economic estimate. *Environ. Res.* **2019**, *172*, 475–485. [[CrossRef](#)]
19. Thompson, V.; Kennedy-Asser, A.T.; Vosper, E.; Eunice-Lo, Y.T.; Huntingford, C.; Andrews, O.; Collins, M.; Hegerl, G.C.; Mitchell, D. The 2021 western North America heat wave among the most extreme events ever recorded globally. *Sci. Adv.* **2022**, *8*, eabm6860. [[CrossRef](#)] [[PubMed](#)]
20. White, R.H.; Anderson, S.; Booth, J.F.; Braich, G.; Draeger, C.; Fei, C.; Harley, C.; Henderson, S.B.; Jakob, M.; Lau, C.A.; et al. The unprecedented Pacific Northwest heatwave of June 2021. *Nat Commun.* **2023**, *14*, 727. [[CrossRef](#)] [[PubMed](#)]
21. Russo, S.; Sillmann, J.; Fischer, E. Top ten European heatwaves since 1950 and their occurrence in the coming decades. *Environ. Res. Lett.* **2015**, *10*, 124003. [[CrossRef](#)]
22. Vautard, R.; Van Aalst, M.; Boucher, O.; Drouin, A.; Haustein, K.; Kreienkamp, F.; Van Oldenborgh, G.J.; Otto, F.; Ribes, A.; Robin, Y.; et al. Human contribution to the record-breaking June and July 2019 heatwaves in Western Europe. *Environ. Res. Lett.* **2020**, *15*, 094077. [[CrossRef](#)]
23. Lhotka, O.; Kyselý, J. The 2021 European heat wave in the context of past major heat waves. *Earth Sci.* **2022**, *9*, e2022EA002567. [[CrossRef](#)]
24. Olivares-Navarro, C. Climatología en Asturias en el periodo 1981–2010. Master's Thesis, Universidad de Oviedo, Oviedo, Spain, 2015.
25. Agencia Estatal de Meteorología. *Informe Sobre el Estado del Clima en España en 2023*; Ministerio para la Transición Ecológica y el Reto Demográfico—Gobierno de España: Madrid, Spain, 2024. [[CrossRef](#)]
26. Olcina-Cantos, J.; Martí-Talavera, J.; Sánchez-Almodóvar, E. Evolución reciente de precipitación y temperatura en la región mediterránea de la Península Ibérica: Revisando la señal del calentamiento global a escala regional. *Cuad. Geográficos Univ. Granada* **2024**, *63*, 51–73. [[CrossRef](#)]
27. IPCC. Resumen para responsables de políticas. In *Climate Change 2021: The Physical Science Basis. Contribution of Working Group I to the Sixth Assessment Report of the Intergovernmental Panel on Climate Change*; Masson-Delmotte, V., Zhai, A., Pirani, S., Connors, C., Péan, S., Berger, N., Caud, Y., Chen, L., Goldfarb, M.L., Gomis, M., et al., Eds.; Cambridge University Press: Cambridge, UK, 2021; Available online: [https://www.ipcc.ch/report/ar6/wg1/downloads/report/IPCC\\_AR6\\_WG1\\_SPM\\_Spanish.pdf](https://www.ipcc.ch/report/ar6/wg1/downloads/report/IPCC_AR6_WG1_SPM_Spanish.pdf) (accessed on 22 November 2023).

28. Lu, R.; Xu, K.; Chen, R.; Chen, W.; Li, F.; Lv, C. Heat waves in summer 2022 and increasing concern regarding heat waves in general. *Atmos. Ocean. Sci. Lett.* **2023**, *16*, 100290.
29. León-Gómez, I.; Gómez-Barroso, D.; Larrauri, A. Informe MoMo. Excesos de Mortalidad por Todas las Causas y Atribuibles a Excesos de Temperatura en España. 16 de Mayo al 30 de Septiembre de 2023. Centro Nacional de Epidemiología. 2023. CIBERESP. ISCIII. Available online: <https://repisalud.isciii.es/rest/api/core/bitstreams/74f2e420-be42-4b5b-907e-e203ef8abb0d/content> (accessed on 25 November 2023).
30. Alló, M.; Loureiro, M. Análisis de la evolución del sentimiento hacia el cambio climático en España. In *Big Data. Predicción y Decisiones Económicas con Big Data*; Peña, D., Poncela, P., Senra, E., Eds.; Funcas: Madrid, Spain, 2023; pp. 33–51.
31. López-García, J.D.; Carvajal-Escobar, Y.; Enciso-Arango, A.M. Sistemas de alerta temprana con enfoque participativo: Un desafío para la gestión del riesgo en Colombia. *Luna Azul* **2017**, *44*, 231–246. [CrossRef]
32. Robine, J.M.; Cheung, S.L.K.; Le Roy, S.; Van Oyen, H.; Griffiths, C.; Michel, J.P.; Herrmann, F.R. Death toll exceeded 70,000 in Europe during the summer of 2003. *Comptes Rendus Biolog.* **2008**, *331*, 171–178. [CrossRef]
33. Alomar-Garau, G.; Llop-Garau, J. La isla de calor urbana de Palma (Mallorca, Islas Baleares): Avance para el estudio del clima urbano en una ciudad litoral mediterránea. *Bol. Asoc. Geogr. Esp.* **2018**, *78*, 392–418. [CrossRef]
34. Santos-Burguete, C.; Subías Díaz-Blanco, A.; Roa Alonso, A. *Recuperación de la clasificación sinóptica de Font: Reconstrucción con el reanálisis ERA40*; Agencia Estatal de Meteorología, Madrid. Ministerio para la Transición Ecológica. Catálogo de Publicaciones de la Administración General del Estado: Madrid, Spain, 2019.
35. Rantanen, M.; Laaksonen, A. The jump in global temperatures in September 2023 is extremely unlikely due to internal climate variability alone. *Npj Clim. Atmos. Sci.* **2024**, *7*, 34. [CrossRef]
36. Rodríguez-Ballesteros, C. ¿Son los Veranos en España Cada vez Más Largos? 2018. Available online: <https://climaenmapas.blogspot.com/p/durverano.html> (accessed on 30 November 2023).
37. Lemus-Canovas, M.; Insua-Costa, D.; Trigo, R.M.; Miralles, D.G. Record-shattering 2023 Spring heatwave in western Mediterranean amplified by long-term drought. *Npj Clim. Atmos. Sci.* **2024**, *7*, 25. [CrossRef]
38. Núñez-Mora, J.Á. Una Primera Aproximación Climática al Extraordinario Calor del 13 y 14 de Mayo de 2015. *Meteociencia* **2016**, 4–5. Available online: [https://repositorio.aemet.es/bitstream/20.500.11765/11820/1/Primera\\_aproximacion\\_Mora.pdf](https://repositorio.aemet.es/bitstream/20.500.11765/11820/1/Primera_aproximacion_Mora.pdf) (accessed on 30 November 2023).
39. Tomczyk, A.M.; Bednorz, E.; Połnolniczak, M. The occurrence of heat waves in Europe and their circulation conditions. *Geografie* **2019**, *124*, 1–17. [CrossRef]
40. García-Herrera, R.; Díaz, J.; Trigo, R.M.; Hernández, E. Extreme summer temperatures in Iberia: Health impacts and associated synoptic conditions. *Ann. Geophys.* **2005**, *23*, 239–251. [CrossRef]
41. Stendel, M.; Francis, J.; White, R.; Williams, P.D.; Woollings, T. The jet stream and climate change. In *Climate Change*; Elsevier: Amsterdam, The Netherlands, 2021; pp. 327–357.
42. Arrillaga, J.A.; Yagüe, C.; Sastre, M.; Román-Cascón, C. Evaluación de las Características de la Brisa Marina en la Costa Cantábrica Oriental Mediante Observaciones y Simulaciones con el Modelo WRF. In Proceedings of the XXXIV Jornadas Científicas de la Asociación Meteorológica Española, Teruel, Spain, 29 February–2 March 2016; AEMET, 2016. Available online: <https://repositorio.aemet.es/bitstream/20.500.11765/6107/1/xxxivjornadasame-evaluacionbrisamarinacantabricowrf.pdf> (accessed on 3 December 2023).
43. Hernández-Holgado, O. Formación de Nieblas Marinas y su Transformación en Estratos. *Acta De Las Jorn. Científicas De La Asoc. Meteorológica Española* **2006**, 29. Available online: [https://repositorio.aemet.es/bitstream/20.500.11765/11568/1/Hernandez\\_Holgado.pdf](https://repositorio.aemet.es/bitstream/20.500.11765/11568/1/Hernandez_Holgado.pdf) (accessed on 10 December 2023).
44. Espín-Sánchez, D.; Olcina-Cantos, J. Changes in the Climate Comfort of the Coast of Spain (1940–2022). *Geogr. Res. Lett.* **2024**, *50*, 45–67. [CrossRef]
45. Zhao, L.; Oppenheimer, M.; Zhu, Q.; Baldwin, J.W.; Ebi, K.L.; Bou-Zeid, E.; Guan, K.; Lu, X. Interactions between urban heat islands and heat waves. *Environ. Res. Lett.* **2018**, *13*, 034003. [CrossRef]
46. Hidalgo-García, D. Analysis of urban heat island and heat waves using Sentinel-3 images: A study of Andalusian Cities in Spain. *Earth Syst. Environ.* **2022**, *6*, 199–219. [CrossRef]
47. Martín-Vide, J.; Moreno-García, M.C. Probability values for the intensity of Barcelona’s urban heat island (Spain). *Atmos. Res.* **2020**, *240*, 104877. [CrossRef]
48. Kirschner, V.; Mackû, K.; Moravec, D.; Mañas, J. Measuring the relationships between various urban green spaces and local climate zones. *Sci. Rep.* **2023**, *13*, 9799. [CrossRef]
49. Chen, K.; Boomsma, J.; Holmes, H.A. A multiscale analysis of heatwaves and urban heat islands in the western US during the summer of 2021. *Sci. Rep.* **2023**, *13*, 9570.
50. Fernández-García, F. El clima urbano de Madrid y su influencia sobre el confort térmico. *Bol. R. Soc. Geogr.* **2002**, *138*, 169–185.
51. Fernández-García, F.; Rasilla, D. Olas de calor e influencia urbana en Madrid y su área metropolitana. *Estud. Geogr.* **2008**, *265*, 495–518. [CrossRef]

52. Rasilla, D.; Allende-Álvarez, F.; Fernández-García, F. *La isla de Calor Urbano de Madrid Durante la ola de Calor de Julio 2015*; X Congreso Internacional AEC: Clima, sociedad, riesgos y ordenación del territorio: Madrid, Spain, 2016. [[CrossRef](#)]
53. Rasilla, D.; Allende-Álvarez, F.; Martilli, A.; Fernández-García, F. Heat Waves and Human Well-Being in Madrid (Spain). *Atmosphere* **2019**, *10*, 288. [[CrossRef](#)]
54. Lemus-Canocas, M.; Martin-Vide, J.; Moreno-Garcia, M.C.; Lopez-Bustins, J.A. Estimating Barcelona's metropolitan daytime hot and cold poles using Landsat-8 Land Surface Temperature. *Sci. Tot. Environ.* **2020**, *699*, 134307. [[CrossRef](#)]
55. Marti, A.; Royé, D. Intensidad y duración del estrés térmico en verano en el área urbana de Madrid. *Geographicalia* **2021**, *73*, 95–113. [[CrossRef](#)]
56. Cuadrat, J.M.; Serrano-Notivoli, R.; Barrao, S.; Saz, M.Á.; Tejedor, E. Variabilidad temporal de la isla de calor urbana de la ciudad de Zaragoza (España). *Geogr. Res. Lett.* **2022**, *48*, 97–110. [[CrossRef](#)]
57. Olcina-Cantos, J.; Serrano-Notivoli, R.; Miró, J.; Meseguer-Ruiz, O. Tropical nights on the Spanish Mediterranean coast, 1950–2014. *Clim. Res.* **2019**, *78*, 225–236. [[CrossRef](#)]
58. Royé, D.; Martí-Ezpeleta, A. Análisis de las noches tropicales en la fachada atlántica de la Península Ibérica. Una propuesta metodológica. *Bol. Asoc. Geogr. Esp.* **2015**, *69*, 351–368.
59. Royé, D. The effects of hot nights on mortality in Barcelona, Spain. *Int. J. Biometeorol.* **2017**, *61*, 2127–2140. [[CrossRef](#)] [[PubMed](#)]
60. Royé, D.; Sera, F.; Tobías, A.; Lowe, R.; Gasparrini, A.; Pascal, M.; de'Donato, F.; Nunes, B.; Teixeira, J.P. Effects of Hot Nights on Mortality in Southern Europe. *Epidemiology* **2021**, *32*, 487–498. [[CrossRef](#)] [[PubMed](#)]
61. Damiens, F.; Lott, F.; Millet, C.; Plougonven, R. An Adiabatic Foehn Mechanism. *Q. J. Roy. Meteorol. Soc.* **2018**, *144*, 1369–1381. [[CrossRef](#)]
62. Jansing, L.; Sprenger, M. Thermodynamics and airstreams of a south foehn event in different Alpine valleys. *Q. J. Roy. Meteorol. Soc.* **2022**, *148*, 2063–2085. [[CrossRef](#)]
63. Yoon, D.; Cha, D.H.; Lee, G.; Park, C.; Lee, M.I.; Min, K.H. Impacts of synoptic and local factors on heat wave events over southeastern region of Korea in 2015. *J. Geophys. Res. Atmos.* **2018**, *123*, 12081–12096. [[CrossRef](#)]
64. Nishi, A.; Kusaka, H. Effect of foehn wind on record-breaking high temperature event (41.1 °C) at Kumagaya on 23 July 2018. *Sola* **2019**, *15*, 17–21. [[CrossRef](#)]
65. González-Herrero, S.; Barriopedro, D.; Trigo, R.M.; López-Bustins, J.A.; Oliva, M. Climate warming amplified the 2020 record-breaking heatwave in the Antarctic Peninsula. *Commun. Earth Environ.* **2022**, *3*, 122. [[CrossRef](#)]
66. García-Hernández, C. Los temporales de nieve de 1888 en Asturias: Respuesta social e institucional. *Investig. Geogr.* **2019**, *71*, 97–117. [[CrossRef](#)]

**Disclaimer/Publisher's Note:** The statements, opinions and data contained in all publications are solely those of the individual author(s) and contributor(s) and not of MDPI and/or the editor(s). MDPI and/or the editor(s) disclaim responsibility for any injury to people or property resulting from any ideas, methods, instructions or products referred to in the content.